Mémoire

Auteur : Noville, Youri
Promoteur(s) : 879; Cudell, Jean-Rene
Faculté : Faculté des Sciences
Diplôme : Master en sciences physiques, à finalité approfondie
Année académique : 2020-2021
URI/URL : http://hdl.handle.net/2268.2/12234

Bose-Einstein Condensate of axions

Youri Noville

A dissertation presented in partial fulfilment of the requirements for the Degree of Master of Science in Physics

Academic year 2020-2021

To Louise,
who too early left the Stage

Acknowledgements

This year was a long journey through Physics and Life and it is now time to thank those without whom this work would not exist. My thoughts go firstly to my two promoters, Prof. Peter Schlagheck and Prof. Jean-René Cudell, for their help, our (quasi) weekly meetings, and our numerous discussions about Physics. They believed in this thesis when I was not, even if they do not know it. Secondly, I would like to express my sincere gratitude to my Thesis Reading Committee: Prof. John Martin, Prof. Matthieu Verstraete and Prof. Geoffroy Lumay. You have accepted to read this work and I hope you will enjoy it.

My thanks then go to my family, which had to live with myriads of sheets spread across the house. I also wish to thank my dear friends Pierrick Verwilghen, Matteo Leonard and Tom Weelen for those five years, and especially Simon Dengis for his encouragement and our evenings spent talking about our Universe and Its Laws. Finally I should thank all the people that helped me to reach the end of my master's degree.

Contents

Introduction

Motivation

One of the greatest achievements of humankind, with art, is maybe science. For centuries, humanity has strived for a better understanding of our Universe. If it was at first by invoking mythological ideas such as gods and chimeras, we soon developed the basis of what will become the scientific method. One of those big questions is the nature of matter. At the birth of the twentieth century, two new theories questioned our perception of concepts such as time, space, and matter: general relativity and quantum theory. The former helped us to dive into the nature of spacetime, solving puzzles such as the precession of the perihelion of Mercury or the medium carrying electromagnetic waves. The latter shook our perception of reality, slaying concepts such as particle, position, and determinism. Both theories were still partially understood and the next decades were rich in discoveries and counter-intuitive phenomena.

In the second half of the century, what we now call the Standard Model of Particle Physics (SM) began to emerge. Accelerators and cosmic rays allowed us to discover a total of thirty elementary particles: twelve leptons and anti-leptons, twelve quarks and anti-quarks, and five bosons, carriers of three fundamental interactions. The last particle of the Standard Model, the Higgs Boson, predicted in the sixties, was found much later, in 2012.

If the Standard Model seems to work exceptionally well, it cannot explain everything. Indeed, some parameters such as the number of generations of leptons or the different mixing angles are unexplained. Experiments such as Muon g-2 hint at Physics beyond the Standard Model. Moreover, 95% of the content of our Universe is not encompassed by the SM: dark energy, probably accountable for the expansion of the universe and dark matter, which, as we will see in Chapter 1, cannot be neglected.

All these unanswered questions lead to a legitimate interrogation: may new undetected particles exist? Plenty of theories predict a plethora of those. One of them, well-studied and imagined by Frank Wilczek [2] is the axion, an ultralight particle that could be born from a broken symmetry of the strong interaction. The idea is that if clouds of axions have reached a sufficiently low temperature, due to their huge Compton wavelength and their bosonic statistic, they could form a Bose-Einstein condensate. We are then left with the following question: what would be the observational consequences of such condensates of axions, and could those condensates explain dark matter?

Plan and goals of the thesis

The goal of this Master thesis is to study the hypothetical Bose-Einstein condensation (BEC) of axions and its effect on galaxies. To reach this goal, we will first introduce the dark matter problem. A brief history will be given as well as some evidence of its

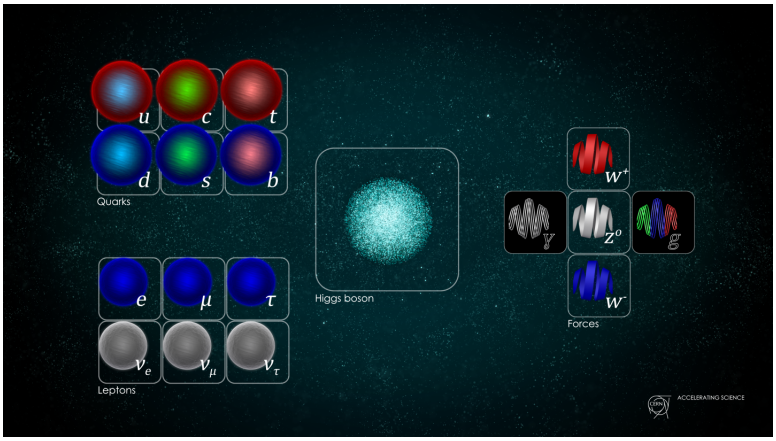

Figure 1: The Standard Model of Particles and its wealth of 30 particles: 6 quarks and their associated anti-quarks, six leptons and their anti-twins as well as six bosons, carriers of three fundamental interactions. Image taken from [1].

existence. The second half of the first chapter will be devoted to the candidates for dark matter and further study of the axions: how could they have appeared, why and what are their main properties. We will also talk about ALPs, axion-like particles, which appear in theories beyond the Standard Model. Chapter 2 will present the theory behind Bose-Einstein condensation in its full glory. We will discuss the conditions required to achieve Bose-Einstein condensation, the description of a condensate as well as the excitations that may appear in such a structure. This chapter will allow us to apply the BEC theory to a cloud of axions. Chapter 3 will start with some reminders about quantum field theory. Then, the self-interaction of axions will be studied and the consequences of this interaction. Finally, we will try to describe a BEC of axions in different configurations.

Chapter 4 will step in the real world and compare our model to observations. The first test for a dark matter model is the rotation curves of galaxies and we shall thus confront our equations with data from the SPARC database, a catalogue of high-quality rotation curves for 175 galaxies. The last chapter of this thesis will discuss our results, try to explain the eventual divergences between theory and observations, and draw adequate conclusions. We will also provide ideas and suggest further possible investigations.

Units and conventions

We will be dealing in this work with two very different mass and size scales. On the one hand, we will be studying particles and Bose-Einstein condensates. On the other hand, we will look at galactic-size structures. It may thus be difficult to choose the right system of units and one is doomed to live with order of magnitudes strolling around the calculations. For the sake of clarity and simplicity [1], we chose to use natural units such that

$$c = \hbar = k_B = 1 \tag{1}$$

where $\hbar$ is the reduced Planck's constant and k_B the Boltzmann constant. As a consequence, we will work with only one unit, the electron-volt. Since we should compare our

[1] It is easier to remove a $\hbar$ than keeping track of all constants.

theoretical model to observation at the end of this thesis, one could argue that this is not a wise choice. To ease conversion and understanding of this work, we shall thus grant the reader with a conversion table for units and for the Cavendish constant G.

Conversion of Natural Units in SI	
Energy	$1\text{ eV} = 1.6\,10^{-19}$ J
Mass	$1\text{ eV} = 1.8\,10^{-36}$ kg
Length	$1\text{ eV}^{-1} = 2.0\,10^{-7}$ m
Time	$1\text{ eV}^{-1} = 6.6\,10^{-16}$ s
Temperature	$1\text{ eV} = 1.2\,10^{13}$ K

This table will allow us to convert our astrophysical units into natural units. For instance, one has

$$1\text{ pc} = 3.08\,10^{16}\text{ m} = 1.57\,10^{23}\text{ eV}^{-1} \tag{2}$$

An important point to remember concerns velocity. Since $c = 1$, velocities are dimensionless and will be expressed as fraction of c. As another example, one can convert the Cavendish constant into natural units.

$$G = 6.67\,10^{-11}\text{ m}^3\text{ kg}^{-1}\text{ s}^{-2} = 6.98\,10^{-57}\text{ eV}^{-2} \tag{3}$$

We shall now remind the reader of some usual notations used in this work. A scalar number will be denoted by a plain letter such as a. For three-dimensional vectors, we will use bold letters.

$$\boldsymbol{r} = (r_1, r_2, r_3) \tag{4}$$

For operators, we use the usual notation $\hat{O}$. We will make use of general relativity in some parts of this thesis as well as quantum field theory. In this context, Greek indices such as μ will vary between 0 and 3 while Latin indices like i will vary between 1 and 3 if not otherwise mentioned. Four-vectors will be written as

$$U^\alpha = \left(U^0, U^1, U^2, U^3\right) \tag{5}$$

We shall also introduce the well-known Einstein convention for summation

$$p_\alpha q^\alpha = p_0 q^0 + p_1 q^1 + p_2 q^2 + p_3 q^3 \tag{6}$$

For a function depending of the coordinates, one should use parentheses. For a functional, one will preferably use squared brackets. For instance, the action of a scalar field depending of x^μ will be written as

$$S\left[\phi\right] = S\left[\phi(x^\mu)\right] \tag{7}$$

Scalar product in curved space-time will be defined as

$$g_{\mu\nu} x^\mu y^\nu = x_\nu y^\nu \tag{8}$$

where $g_{\mu\nu}$ stands for the metric tensor. The author of this work decided to follow the "general relativity" convention for the signature of the metric tensor i.e. the $(-+++)$ convention, also called the East Coast metric. Particle physicists often use the $(+---)$

convention. However, for different technical reasons [3], we should prefer the first one. For instance, the flat Minkowski space-time will be described by the usual metric

$$g_{\mu\nu} = \begin{pmatrix} -1 & 0 & 0 & 0 \\ 0 & 1 & 0 & 0 \\ 0 & 0 & 1 & 0 \\ 0 & 0 & 0 & 1 \end{pmatrix} \tag{9}$$

Following this prescription, the interval element will be given by

$$ds^2 = g_{\mu\nu} dx^\mu dx^\nu \tag{10}$$

1

Very light particles and the Dark Matter Problem

Before asking ourselves what dark matter really is and beginning to devise complex and intricate theories about it, it seems wise and discerning to brush firstly a brief history of the main discoveries and hints that led to the concept of dark matter. Indeed, a deep understanding of the problem can only be achieved by a well-suited contextualisation of the topic. The goal here will not be to paint an exhaustive review of the field but rather to introduce the main evidence for the existence of dark matter, its historical origin and what it tells us about the nature of dark matter. A more thorough historical review of the topic can be found in [4–6].

The first section of this chapter will be based mainly on those articles and will present the early evidence in favour of dark matter. We will then discuss in greater details the rotation curves of galaxies since we will use this phenomenon to test the model presented in this master thesis. Following that, we will talk about some cosmological evidence such as structure formation or the baryonic content of the Universe, essential to understand the complexity of the dark matter issue. Finally, the different candidate solutions to the dark matter problem will be briefly presented. We will justify our choice in favour of axions or others very light particles and their main properties will be developed in more depth.

1.1 The need for Dark Matter

As mentioned above, it seems wise to begin by analysing the different pieces of evidence in favour of dark matter. The following sections will be mostly a qualitative description. More accurate data concerning dark matter such as its average density in galaxies or in the Universe and its precise ratio between baryonic matter and dark matter will be mentioned when needed.

1.1.1 Early evidence

The idea of an invisible matter affecting the usual baryonic and luminous matter is not new. Since the eighteenth century, the idea of dark stars possessing an escape velocity greater than the speed of light was raised by Laplace and Michell. If their concept of what we now call black holes was still very primitive and did not imply radical modification of

concepts such as space and time, this idea of invisible bodies lurking in the heavens can be seen as a kind of primitive dark matter. However their hypotheses were at that time only theoretical and did not rely on any observational fact. One had to wait until the dawn of the twentieth century to see in experimental data the hypothetical existence of "dark matter".

This first evidence came from measurements of the matter density in the surrounding of our solar system notably made by Lord Kelvin in 1904 and Oort in 1932 among others [7, 8]. Quite surprisingly, they concluded that the amount of dark matter, which they believed composed of faint stars and gas, was at most of the same order of magnitude as the amount of visible matter. The first serious hint in favour of greater quantities of dark matter is the study by Fritz Zwicky of the Coma cluster, some 99 Mpc ($\sim 3\,10^{24}$ m) away from Earth, concerning the red-shifts of galaxies in his seminal article of 1933 [9]. Zwicky's idea was fairly simple. He began by deriving the observed velocities of the galaxies by mean of their redshifts. Then, assuming that the cluster had reached a mechanical stationary state, was of spherical shape and composed of more or less 800 nebulae of 10^9 solar masses ($\sim 2\,10^{39}$ kg), he used the virial theorem stating that

$$\langle E_k \rangle = \frac{1}{2}\langle E_p \rangle \tag{1.1}$$

to find what should be the observed velocities of the galaxies. He then reached the conclusion that the Coma cluster was 400 time heavier than one would expect if only composed of luminous matter. Although further studies would reduce the estimated amount of dark matter some 90%, one could not escape the qualitative conclusion of Zwicky: a large amount, in fact most of the matter, was invisible to our instruments. This first observation was corroborated by the study of 60 galaxies by Vera Rubin nearly 40 years later. As she considered the hydrogen and helium presents in those galaxies, Rubin obtained the rotation velocity of the studied galaxies as a function of the radius. While one should expect a decreasing velocity far from the galactic bulge, a Keplerian behaviour, the rotation curves remain flat as if an important cloud of invisible matter was present.

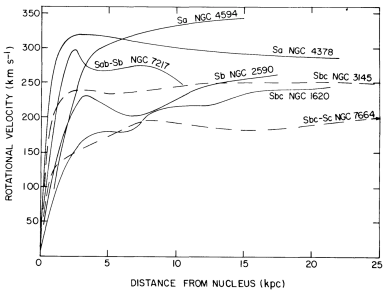

Figure 1.1: Rotation curves of seven galaxies taken from the Rubin article [10].

1.1.2 Gravitational lensing of galaxy clusters

Maybe one of the most striking pieces of evidence in favour of general relativity (GR) was the famous observation made by Eddington in 1919 of a solar eclipse. GR predicted that since the energy-moment tensor is able to curve space, one should be able to observe a

star hidden behind the sun due to the curved geodesic followed by the emitted photons[1]. It was indeed observed. This concept of curved space-time led to the idea of gravitational lensing. If matter can bend the trajectory of light as a glass lens can[2], then one should be able to witness such lensing caused by very massive objects. The solutions for the trajectories of photons just require basics of GR. Starting from the metric outside a spherical body, it is straightforward to deduce two first integrals from the Lagrangian and conclude by computing the geodesic of photons. However the calculation is not needed here and we will only emphasise what lensing can teach us about dark matter.

Firstly discovered in 1979 [11], lensing soon opened the doors to numerous astrophysical observations, notably through the lensing of galaxy clusters. Since it allows to measure precisely masses independently of the kind of matter (baryonic or dark) [12], it can be combined with others methods to evaluate the ratio between the usual baryonic matter and the dark one (for the baryonic contribution, one of the most simple methods is the direct observation of the cluster luminosity).

1.1.3 Hydrostatic equilibrium of clusters

Another method to weight galaxy clusters is by observing them at the x-ray wavelength. Actually the x-rays luminosity L depends on the electron number density, which can thus be inferred from the measured L. Furthermore, the intensity of the emission rays from a cluster informs us about its temperature. Since the pressure depends on both quantities [13], one can use the equation for a cluster having reached hydrostatic equilibrium

$$\frac{dp}{dr} = -G\frac{M\rho_{gas}}{r^2} \tag{1.2}$$

to obtain a measurement of the total mass of the cluster. For instance, the Chandra and XMM-Newton satellites observations led to a baryonic to dark matter ratio of 1/6.

1.1.4 Rotation curves of galaxies

As mentioned in a previous section, one of the earliest and most striking proofs of the existence of dark matter has been the rotation curves of the galaxies. Following the study of Rubin and her collaborators, more galaxies were observed to confirm the observations. One of the most recent ones is the database made by the SPARC team that used the Spitzer Space telescope by observing the H1 and Hα emission lines of hydrogen [14]. Those data will be used in Chapter 4 to test our model.

While rotation curves allow us to compute the dark matter density inside galaxies, the asymptotic velocities give us another important insight into the dark matter problem. In 1977, Tully and Fisher computed those asymptotic velocities and made a capital discovery: the Tully-Fisher relation. They found that the asymptotic rotational velocities of galaxies were linked to their intrinsic luminosity [15]. Furthermore, it was shown that plotting the asymptotic velocity as a function of the mass of baryonic matter in the

[1] In fact, Newtonian Gravity also predicts a deviation of light-ray. The true difference is that the GR predicts a deviation twice as large as the Newtonian one.

[2] One should however note that, if the effects are comparable, the fundamental nature of the lensing is rather different. While the glass lens reorients a light beam, a large mass really bends space-time, modifying the geometry in its surrounding.

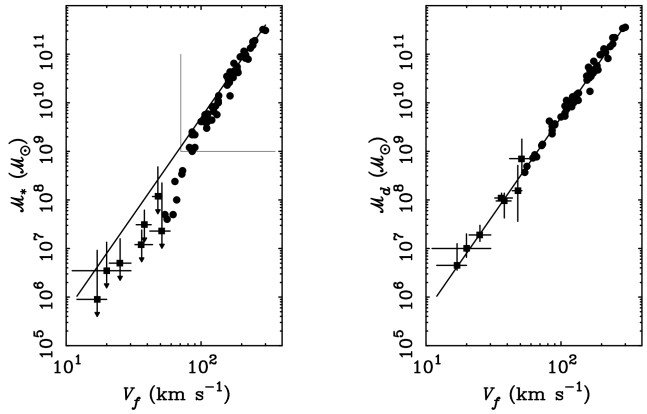

Figure 1.2: On the left panel, the stellar mass Tully-Fisher relation, directly derived from the intrinsic luminosity Tully-Fisher relation. On the right panel, the baryonic Tully-Fisher relation presenting a better fit. The v_f stands for the final velocity of the rotation curves while the M_* and the M_d stand for the total stellar mass and the total baryonic mass. Figure taken from [16]

galaxy gives even stronger constraints on the relation between the quantity of baryonic matter and dark matter in galaxies [16, 17] as can be seen on Figure 1.2. It is important to understand at this point that the Tully-Fisher relation should not be regarded as anecdotal. One could expect that the quantity of dark matter in a galaxy is more or less linked to the quantity of baryonic matter, which seems obvious. However this relation tells more than that. It tells us that from the mass of the baryonic matter in a galaxy, it is straightforward to know the total mass of dark matter in this galaxy. The baryonic matter seems to be a sufficient parameter to give the amount of dark matter. Therefore the Tully-Fisher relation provides a deep link between the two kinds of matter. In fact, this peculiar relation gave birth to an other hypothesis: the non-existence of dark matter and the need to modify the theory of gravity itself.

We now discuss the different types of galaxies and give some numbers concerning their structures to get an idea of the order of magnitude involved. We may class galaxies following the Hubble classification, which relies on their appearance. The four main kinds of galaxies are elliptical, spiral, barred spiral and irregular. Each of these categories is then subdivided into multiple types depending on their bulge and their eventual arms as is shown in Figure 1.3. We will restrict our study to galaxies that are at least cylindrically axisymmetric and present in the SPARC database i.e. galaxies of types SO, Sa, Sb and Sc. The corresponding shapes are shown in Figure 1.3. The SPARC data will be further discussed in Chapter 4.

Galaxies come in all shapes and forms. They differ by their ages, their sizes, their masses and it is difficult to precisely give a general description. We will thus try to fix the order of magnitude by looking at a well-known galaxy, the Milky Way. A typical spiral galaxy may be separated into three main parts: a bulge, a disk and a spherical halo, as can be seen in Figure 1.4. The Milky Way weights between $0.8\,10^{12}$ solar masses. The bulge accounts for more or less 10^{10} solar masses. The disk weights six times more. Most of the galaxy mass is composed of dark matter with nearly $70\,10^{10}$ solar masses.

Concerning distance scale, the Bulge is 2 kpc wide, or $3.14\,10^{26}$ eV^{-1}. The diameter

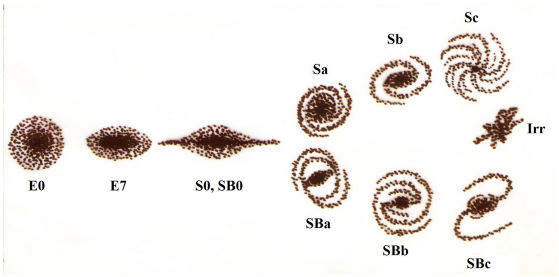

Figure 1.3: The "Hubble fork", the classification introduced in 1926 by E. Hubble [18].

of the disk measures around $78.5\,10^{26}$ eV^{-1} while the dark matter halo can extend up to $3.14\,10^{28}$ eV^{-1}.

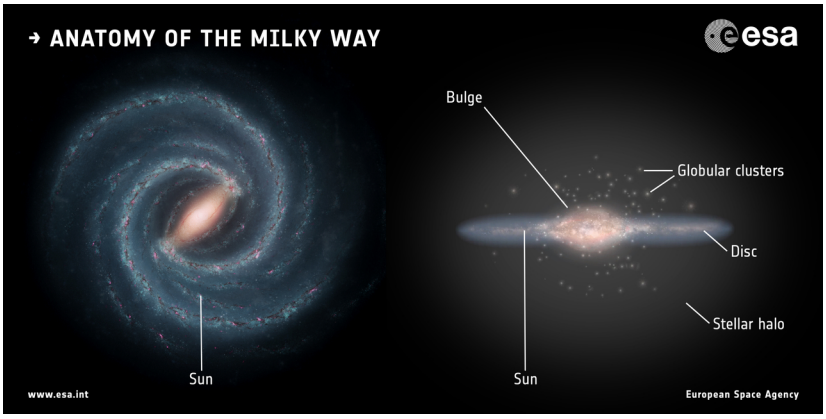

Figure 1.4: The structure of our Milky Way, a typical spiral galaxy [19].

1.1.5 Cosmological evidence

Even if the first evidence for dark matter came from rotation curves of galaxies and their dynamics, we now have more stringent constraints coming from Cosmology. Indeed, dark matter left during the early days of our Universe its fingerprint in the Cosmic Microwave Background (CMB). By studying the anisotropies in it, one is able to highlight the necessity for dark matter. Furthermore, the formation of large-scale structures, influenced by gravity, is highly influenced by the mass content of our Universe and thus dark matter.

Some Cosmology reminders

We first recall some basics of cosmology. It will allow us to review the cosmological evidence for dark matter as well as the birth of axions and ALPs during the early universe. The geometrical structure of spacetime is described by the metric tensor $g_{\mu\nu}$. Choosing an arbitrary system of coordinates x^μ, the interval, which is our Lorentz-invariant notion of distance, is defined as

$$ds^2 = g_{\mu\nu} dx^\mu dx^\nu \tag{1.3}$$

If one particularises this interval for an isotropic and homogeneous 3D space, one may choose the FLRW metric

$$ds^2 = -dt^2 + a(t)\left(\frac{1}{1-kr^2}dr^2 + r^2 d\theta^2 + r^2 \sin^2\theta d\phi^2\right) \tag{1.4}$$

where k characterises the curvature of space:

- $k < 1$: Negatively curved (Open) Universe
- $k = 0$: Flat Universe
- $k > 1$: Positively (Closed) Universe

What are we describing here? If we look closely at the metric above, it seems similar to the Minkowski metric. In fact, we can think of it as a grid of coordinate lines. This metric describes a 3D space expanding with a rate a. If we inject this metric into the Einstein field equations

$$R_{\mu\nu} - \frac{1}{2}g_{\mu\nu}R + \Lambda g_{\mu\nu} = 8\pi G T_{\mu\nu} \tag{1.5}$$

owe obtain the Friedman equation

$$\left(\frac{\dot{a}}{a}\right)^2 = \frac{8\pi G\rho + \Lambda}{3} - \frac{k}{a} \tag{1.6}$$

If one associates a density to the Λ parameter $\rho_\Lambda = \Lambda/8\pi G$, one can rewrite this equation as

$$\left(\frac{\dot{a}}{a}\right)^2 = \frac{8\pi G\rho_{tot}}{3} - \frac{k}{a} \tag{1.7}$$

We directly see that this equation links the content of the universe to its curvature k. Since the results of the Planck collaboration [20] hint at a flat universe[3], we will assume a null value for k. Furthermore, the ratio $\dot{a}/a$, often called the Hubble parameter and written H, can be measured from the recession velocity of galaxies. This allows us to obtain an observational value for ρ_{tot}. We can then define different parameters $\Omega_\gamma, \Omega_{bar}, \Omega_\Lambda$ and Ω_{DM} which are respectively the fraction of photons, baryonic matter, vacuum and dark matter contained in ρ_{tot}. We have from observational grounds:

- $\Omega_{bar} \approx 0.05$
- $\Omega_{DM} \approx 0.25$
- $\Omega_\Lambda \approx 0.70$

Now that general relativity has endowed us with tools to describe the Universe's history, we should use them to introduce evidence in favour of dark matter. Thanks to the Friedman equation, one can rewind the story and predict multiple events, for instance the decoupling of radiation from matter.

CMB anisotropies

The Cosmic Microwave Background was first detected pas Penzias and Wilson in 1964. This radiation was emitted during the decoupling between photons and matter 380000 years after the Big Bang. If this radiation may seem homogeneous at first sight, small anisotropies in the temperature field are observed. The correlation between two points

[3]Technically, the issue is not totally settled and our Universe may be closed [21].

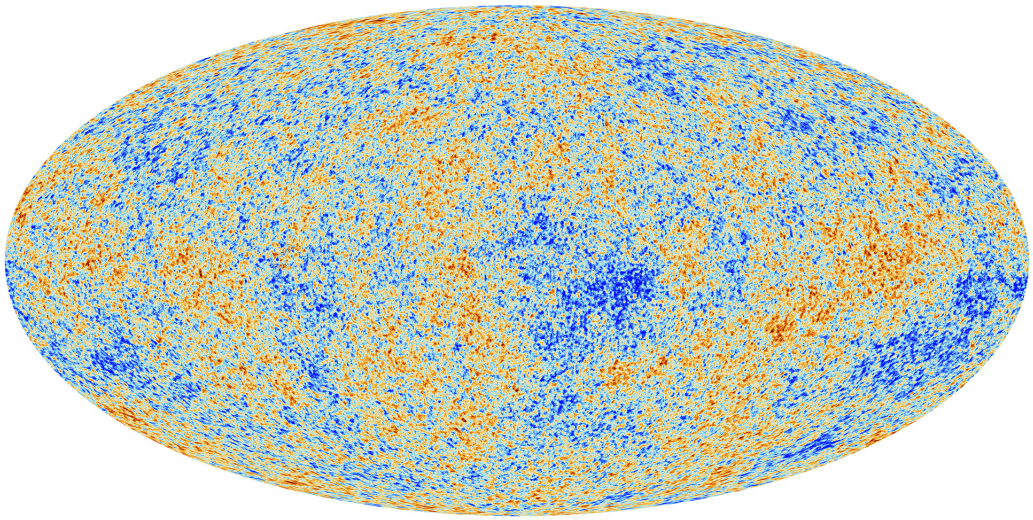

Figure 1.5: The CMB observed by the Planck mission [22]. The temperature fluctuations are caused by small variations in the matter density. Those variations will later give birth to structures such as clusters.

separated by an angle θ may be expressed as [23]

$$C(\theta) = \frac{1}{4\pi} \sum_l (2l+1) C_l P_l(\cos\theta) \tag{1.8}$$

where the P_l are Legendre polynomials and the C_l are coefficients to be determined by observation. Plotting these angular correlations, one obtains various peaks as shown in Figure 1.6. The peaks are due to acoustic waves in the primordial fluid of photons coupled to matter [24]. One would expect those peaks to decline uniformly for wider angles due to dissipation of the acoustic waves. However, even peaks seems to be boosted compared to odd ones. If a comprehensive explanation is out of the scope of this thesis, what we can say is that this spectrum can only be explained by dark matter. MOND theories fail at explaining it. Furthermore those peaks allow us to measure a variety of cosmological parameter such as the total density of the Universe or the ratio between baryonic matter and light.

1.2 Axions and axion-like particles as a solution

1.2.1 Plausible candidates

This master thesis aims at studying axions or ALP's as candidate for dark matter. Other candidates exists and we shall briefly introduce them before developing the theory of the axion. We will try to list here the arguments in favour or disfavour of the different plausible candidates. This discussion will allow the reader to understand why axions are worth studying. To introduce the different candidates, we should first introduce some basic notions about the Standard Model of particle physics. The Standard Model is based gauge theories. This means that the physics underpinning our understanding of nature is described by an action invariant under a local transformation belonging to the group

$$SU(3) \otimes SU(2)_L \otimes U(1)_Y \tag{1.9}$$

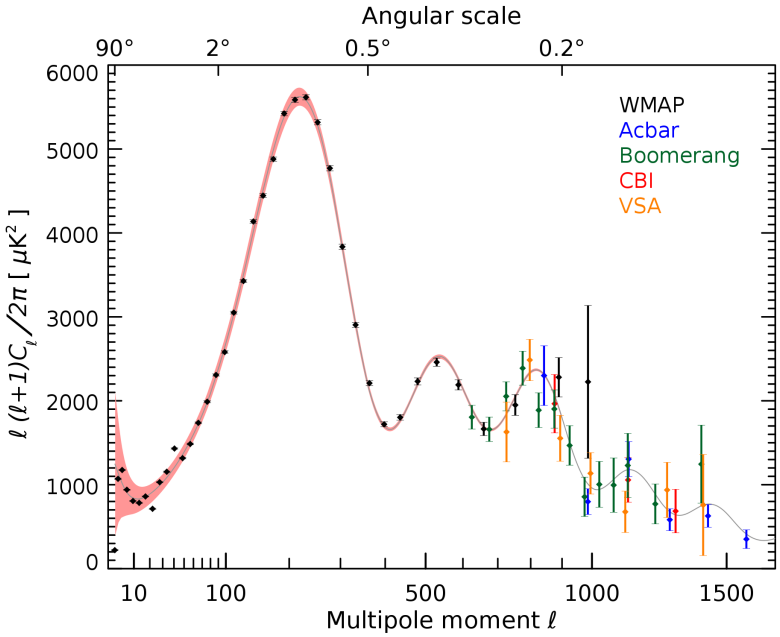

Figure 1.6: Anisotropies spectrum of the CMB [25]. The second peak cannot be explain by MOND theories and requires the existence of matter that does not interact with light, i.e. dark matter.

An example of gauge theory is electromagnetism (EM), for which one can locally perform a transformation on the four-vector potential A^μ without disturbing the underlying physics. Since the gauge can be fixed locally, one may want to compare a physical quantity at two different points and run into a difficulty. We can illustrate this issue with EM and its gauge group U(1), which basically embodies phase changes. For a given field $\psi(x)$, one can decide to change the phase locally:

$$\psi \to \psi' = e^{i\alpha(x)}\psi \tag{1.10}$$

Since this phase is arbitrarly chosen for each value of x, it becomes impossible to compare a quantity between two point x and y. We thus need a new field that will carry the phase between two points. This field, in the case of EM, is the electromagnetic field. Following the same logic with more complex symmetry groups such as $SU(2)$ or $SU(3)$, one sees the emergence of different fields carrying the "phases" of those transformations: eight gluons for $SU(3)$, carriers of the strong interaction and three others bosons for the group $SU(2)$. We will not discuss comprehensively the group $SU(2)_L \otimes U(1)_Y$ mentioned in equation (1.9). We shall just mention that the correct mixing of the associated bosons give rise to the four bosons Z^0, $W^\pm$ and γ.

Apart from those bosons lives a variety of fermions, ruled by the SM Lagrangian (invariant under the group (1.9)). For what we know, there are three generations of leptons

$$\begin{pmatrix}\nu_e\\ e^-\end{pmatrix}\ ,\ \begin{pmatrix}\nu_\mu\\ \mu^-\end{pmatrix}\ ,\ \begin{pmatrix}\nu_\tau\\ \tau^-\end{pmatrix} \tag{1.11}$$

as well as three generations of quarks, fermions that undergo strong interactions.

$$\begin{pmatrix} u \\ d \end{pmatrix} \ , \ \begin{pmatrix} c \\ s \end{pmatrix} \ , \ \begin{pmatrix} t \\ b \end{pmatrix} \tag{1.12}$$

As one can see, those particles are also ruled by certain symmetries and are classified in isospin doublets, which means that the top and bottom particles of each doublet are related to an $SU(2)$ group. Now that we have introduced the main bricks of the SM and the idea of gauge invariance, we are able to discuss the major candidates for dark matter as well as the potential origin of axions and others ALPs.

WIMPs

One of the serious alternatives to axions are WIMPs or Weakly Interacting Massive Particles. WIMPs are hypothetical particles that could have been thermally produced during the early stages of the Universe. The interaction between those particles would be governed by the $SU(2)_L$ bosons and could allow WIMPs to decay, thus explaining the current Dark Matter density [26]. Those particles are especially interesting since they should be found at the weak mass scale, around 250 GeV, which is a scale experimentally reachable. Theoretically speaking, WIMPs naturally arose in extensions of the Standard Model trying to address issues such as the hierarchy problem and well-known Beyond the Standard Model theories such as SUSY, super-symmetry.

Even though they are theoretically relevant and could be at an energy-scale reachable, no detection of WIMPs has been reported yet. Multiple experiments, notably searching for gamma ray excess, are looking for WIMPs and constantly constrain [27] the parameter space for such particles.

Other Exotic Particles

While axions and WIMPs are the main candidates, theorists are a prolific breed and have imagined a wild variety of others candidates. Ranging from Fermi and GUT Balls [28] to Little Higgs theories [29] and sterile neutrinos [30], one could discuss at great length all those particles. The important fact to remember is the following: multiple candidates exist, each having their own flaws and advantages. However none of those candidates has been observed and the energy band where they could hide tends to diminish, leaving the dark matter problem open and intriguing.

1.2.2 The axion and other ALPs

Goldstone's theorem

To explain briefly the origin of the QCD axion and subsequently the origin of ALPs, one has to introduced the Goldstone theorem. Let G be a local symmetry group and $\mathfrak{g}$ its algebra. Next, let $\mathcal{L}$ be a G-invariant Lagrangian density governing the evolution of N scalar fields $\{\phi_i\}$ that can be chosen real without loss of generality. For an infinitesimal transformation of the fields, we have

$$\phi_i \to (1 + i\alpha^a t_a)_{ij}\, \phi_j \tag{1.13}$$

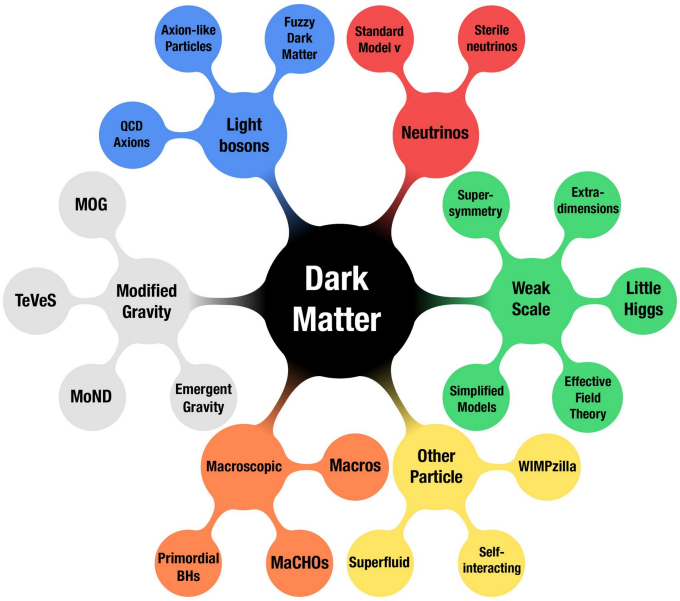

Figure 1.7: What hides behind dark matter? Different candidates exist. Figure taken from [31].

where the t^a are generators of the algebra $\mathfrak{g}$. Then, if we express the Lagrangian as the sum of a kinetic term and a potential term, with $\Phi = (\phi_1, ..., \phi_N)$.

$$\mathcal{L}[\Phi] = K[\Phi] - V[\Phi] \tag{1.14}$$

the Goldstone theorem states the following : each symmetries of $V[\Phi]$ (i.e. transformations belonging to G) that are not symmetries of the vacuum Φ_0 give rise to massless scalar bosons. It is quite simple to verify. First, one can expand the potential term in a power series around the vacuum.

$$V[\Phi] = V[\Phi_0] + (\Phi - \Phi_0)_i \left.\frac{\partial V[\Phi]}{\partial \phi_i}\right|_{\Phi=\Phi_0} + \frac{(\Phi - \Phi_0)_i (\Phi - \Phi_0)_j}{2} \left.\frac{\partial^2 V[\Phi]}{\partial \phi_i \partial \phi_j}\right|_{\Phi=\Phi_0} + \dots \tag{1.15}$$

Since we work at a minimum of $V[\Phi]$, the second term equals zero. Moreover, since the second order term is a quadratic function of the fields, the diagonal elements of the matrix $\left.\frac{\partial^2 V[\Phi]}{\partial \phi_i \partial \phi_j}\right|_{\Phi=\Phi_0}$ contain the information about the masses of the ϕ_i. To continue the proof of the theorem, we look at transformations of the fields that keep the potential term invariant.

$$\phi_i \to \phi_i + \Delta(\Phi)_i : \Delta(\Phi)_i \frac{\partial V[\Phi]}{\partial \phi_i} = 0 \tag{1.16}$$

Thus, we are led to the following condition

$$\Delta(\Phi)_i \frac{\partial^2 V[\Phi]}{\partial \phi_i \partial \phi_i} = 0 \tag{1.17}$$

which evaluated in Φ_0 is fulfilled in two different cases:

- If $\Delta(\Phi_0) = 0$, then $\left.\frac{\partial^2 V[\Phi]}{\partial \phi_i \partial \phi_i}\right|_{\Phi=\Phi_0}$ may be different from zero.

- If $\Delta(\Phi_0) \neq 0$, then $\left.\frac{\partial^2 V[\Phi]}{\partial\phi_i \partial\phi_i}\right|_{\Phi=\Phi_0} = 0$

which concludes the demonstration. If the symmetry is not a perfect symmetry of $V[\Phi]$ but is violated by a small amount, the Goldstone boson cannot rigorously have a null mass and is rather called a "pseudo-Goldstone" boson [32]. The symmetry breaking mechanism and the Goldstone theorem, which we will use to explain the origin of axions and ALPs, is for instance at the core of the BEH mechanism or the explanation of supra-conductivity [33]. In the next sections we will briefly describe how the theorem applies to QCD and other Beyond the Standard-Model theories.

QCD axions

Now that we understand how particles arise from symmetries, we will briefly discuss the origin of the QCD axion, the "primordial" axion. The QCD Lagrangian $\mathcal{L}_{QCD}$ rules the three generations of quarks. In the limit of vanishing masses for quarks, $\mathcal{L}_{QCD}$ exhibits a new symmetry [34]. Since the masses of the up and down quarks are small compared to the strong interaction energy scale Λ_{QCD}, we obtain new symmetries for the following Lagrangian

$$\mathcal{L}^{ud}_{QCD} = -i\bar{u}\gamma^\mu D_\mu u - i\bar{d}\gamma^\mu D_\mu d \tag{1.18}$$

where the covariant derivate D_μ takes into account gauge invariance. Taking the Dirac matrices in the Weyl representation[4], one may rewrite this Lagrangian

$$\mathcal{L}^{ud}_{QCD} = -i\bar{u_L}\gamma^\mu D_\mu u_L - i\bar{d_L}\gamma^\mu D_\mu d_L - i\bar{u_R}\gamma^\mu D_\mu u_R - i\bar{d_R}\gamma^\mu D_\mu d_R \tag{1.19}$$

Apart from the $SU(3)$ symmetry of the Strong Interaction, this Lagrangian is endowed with 4 new symmetries due to the vanishing masses of the up and down quarks:

- $U(1)_V : q \to q' = e^{i\alpha} q$
- $SU(2)_V : Q \to Q' = e^{i\vec{\alpha}\cdot\vec{\sigma}} Q$
- $U(1)_A : q \to q' = e^{i\eta\gamma_5} q$
- $SU(2)_A : Q \to Q' = e^{i\vec{\eta}\cdot\vec{\sigma}\gamma_5} Q$

where V stands for vector and A for axial. The issue is that quark and anti-quark may form condensates of fermions in the vacuum such that

$$\langle u\bar{u}\rangle = \langle d\bar{d}\rangle \approx 300 \text{ MeV}^3 \tag{1.20}$$

Those condensates break the axial symmetries $SU(2)_A$ and $U(1)_A$ [36] and we should thus expect the existence of four particles, three associated with $SU(2)_A$ and one with $U(1)_A$. However, only three of those particles, the pions π^-, π^0 and π^+ are observed. The next scalar particle in the hadronic spectrum is the η but it is too heavy to be a pseudo-Goldstone particle. We thus reach the following conclusion : maybe $U(1)_A$ is not physically a symmetry of the strong interaction although it is a symmetry of (1.19). The solution to this problem came from 't Hooft who showed that the QCD vacuum was more

[4]The reader unfamiliar with Dirac matrices and Quantum Field Theory would perhaps find useful the book from Peskin and Schroeder [35]

complex then expected [37]. He postulated that the true vacuum of the theory was in fact a superposition of vacua

$$|\theta\rangle = \sum_n e^{in\theta} |n\rangle \tag{1.21}$$

where the $|n\rangle$ are different vacua. This is this particular vacuum structure that allows one to add a non-vanishing four divergence to the action and the existence of instantons. The comprehensive study of the instanton effects would not fit into this thesis. The curious reader could be interested in the t'Hooft article cited above. Right now we have done fairly well, but we are not out of the woods. Indeed, the resolution of the $U(1)_A$ problem adds a new term to our Lagrangian

$$\mathcal{L}'_{QCD} = \mathcal{L}_{QCD} + \theta \frac{g^2}{32\pi^2} F_a^{\mu\nu} \tilde{F}_{a\mu\nu} \tag{1.22}$$

where g is the strong interaction coupling constant and $\tilde{F}_{a\mu\nu} = \frac{1}{3}\epsilon_{\mu\nu\alpha\beta}F^{\alpha\beta}$. The $F_a^{\mu\nu}$ fields are the strong interaction equivalents of the $F_{\mu\nu}$ field for Electromagnetism however adapted to non-abelian gauge theories. θ[5] is an unconstrained angle and could thus take any value.

While it seems that we solved our problem, the term in (1.22) violates the CP symmetry, but only by a small amount if the angle θ stays small too. By measuring the neutron electric dipole moment, one can put strong constraints on the value of θ [38]:

$$\theta < 10^{-9} \tag{1.23}$$

This is what is called the strong CP problem and it is at this point of the story that our main actor enters the play. In 1977, Peccei and Quinn proposed a beautiful solution to the strong CP problem [39, 40]. They promoted θ to the vacum expectation value of a field that broke new global chiral symmetry $U(1)_{PQ}$. Technically, adding this broken symmetry consists in adding a dynamical field to our Lagrangian. This dynamical field, which restores the CP symmetry, will be able to "rotate away" the CP-violating term. It was then remarked by Wilczek, that this broken symmetry would give birth to a new pseudo-scalar bosonic particle, the axion. It also implied the addition of interaction term to $\mathcal{L}_{QCD}$, mainly to the electromagnetic field.

Axion-Like Particles

If the QCD axion was introduced to solve the strong CP problem, many theories beyond the Standard Model give birth to axion-like particles. They carry this name due their shared properties with QCD axions. They are pseudoscalar ultralight bosonic particle coupled to the electromagnetic field. For instance, superstring theory sees the emergence of ALPs due to compactification[6] of ten-dimensional massless fields [41]. Moreover, many other extensions of the Standard Model [42, 43] involve broken $U(1)$ symmetries. Since this work does not intend to study a particular ALP but rather their whole family and

[5] Technically, a contribution to θ also come from the re-phasing of the CKM matrix, which rules the flavour mixing between quarks.

[6] Compactification, one of the cornerstone of String Theory, basically consists in wrapping up an infinite dimension (for instance one can imagine a infinite line) into a finite one (we take our previous line and curl it into a circle).

their condensation, it is not useful to discuss those different extensions with much details. One should only remember the general properties of this kind of particles. Indeed, those properties will give rise to a broad range of phenomena, notably the Bose-Einstein condensation of ALPs.

2

The theory of Bose-Einstein Condensation

This chapter will be dedicated to the theoretical study of Bose-Einstein condensate (BEC). First, the theory of BEC of non-interacting particles will be discussed. This will allow us to develop some intuition about this phenomenon and to introduce fundamental concepts. Then, we will pursue by adding trapping and self-interaction to the discussion. Finally, the Gross-Pitaevski and Bogoliubov-de Gennes equations will be studied for some trapping potentials of interest. Since the theory of BEC will not be applied to cold atoms as it is usually the case, particular attention will be made to keep the analysis as general as possible. The Bose-Einstein distribution and the concept of BEC were first introduced by A. Einstein in 1925 [44] following an article of S. Bose about light quantum published in 1924. It is interesting to note that although Einstein correctly deduced the physical consequences of the condensation, he did not believe in its reality. It was not until 1995 that a BEC was observed [45]. Nowadays, a broad literature can be found on the topic and BEC are experimentally well-studied objects. They have even been produced in space [46].

It is rather simple to give an intuitive idea of Bose-Einstein Condensation. Let a gas of N non-interacting bosons, an ideal Bose gas, be in a box of volume L^3. Naively, we have two length scales at our disposal: the inter-particle distance l and the de Broglie wavelength λ_B, given by:

$$l = \frac{L}{N^{1/3}} \tag{2.1}$$

$$\lambda_B = \frac{h}{p} \tag{2.2}$$

Now, let us look at what happens when we lower the temperature. As the system cools down, the momentum of the bosons tends to zero, leading to an overlapping of the de Broglie wavelengths. This overlap of the particles allows us to treat the system as a new object: a condensate. As it will later be shown, the condensation consists in the preferred occupation of a given eigenstate of the Hamiltonian. This intuitive vision of the BEC obviously needs some refinement. It will be necessary to use the many-body formalism.

2.1 Description of many-body quantum systems

In this section, we will introduce the many-body formalism and deduce the equations describing a gas of bosons. As the topic of this master thesis is the BEC of axions, we will consider the case of a number N of indistinguishable scalar particles. Since those particles are indistinguishable and are of bosonic nature, the Hamiltonian of our system is invariant under particle permutations and the wave function describing the N bosons will be fully symmetric in the coordinates of the particles. As we intend to work in a quantum field theory framework, sometimes involving annihilation and creation of particles, the use of a one-particle Hilbert space is not practical. Indeed, if such a space is well-suited to deal with usual non-relativistic quantum mechanics and a fixed number of particles, we should rather introduce the concept of Fock space. Let $\mathcal{H}_n^+$ be the symmetric subset of the n-body Hilbert space $\mathcal{H}_n = \bigotimes_{i=0}^{n} \mathcal{H}$ with $\otimes$ denoting the tensor product of two Hilbert spaces and the $+$ designating the symmetric nature of the space. Then one can define a bosonic Fock space as:

$$\mathcal{F} = \bigoplus_{n=0}^{\infty} \mathcal{H}_n^+ \tag{2.3}$$

with $\oplus$ denoting the direct sum of Hilbert spaces. Defined as above, all the symmetries of our system due to the bosonic nature of the particles are embedded in the concept of Fock space. It seems wise to endow it with a proper basis. Let a basis of a one-body Hilbert space $\mathcal{H}_1$ be given by:

$$\mathcal{B}_1 = \{|\phi_k\rangle\}_{k\in\mathbb{N}_0} \ , \ |\phi_k\rangle : \mathbb{R}^3 \to \mathbb{C} \tag{2.4}$$

Then one can build a basis state for a $\mathcal{H}_n^+$ as follow:

$$|\Phi_{k_1...k_n}\rangle = \frac{1}{\sqrt{n!\prod_{k=0}^{\infty} n_k!}} \sum_{\pi\in\Pi_n} \left|\phi_{k_{\pi(1)}}\right\rangle \otimes ... \otimes \left|\phi_{k_{\pi(n)}}\right\rangle \tag{2.5}$$

where the n_k count the number of times that k appears in the quantum numbers $k_1, ..., k_n$ and Π_n denotes the set of all permutations of n items. Following this definition, it is then trivial to define our Fock basis as:

$$\mathcal{B}_{\mathcal{F}} = \bigoplus_{n=0}^{\infty} \mathcal{B}_n^+ \tag{2.6}$$

where the $\mathcal{B}_n^+$ are the basis composed of states defined as in (2.5). The states composing such a basis are written $|n_0, n_1, ...\rangle$. For instance, the basis state corresponding to two particles in the first quantum state and one particle in the third can be written $|2, 0, 1\rangle$. We can now introduce the annihilation and creation operators as:

$$\begin{cases} \hat{a}_k \,|n_0, n_1, ..., n_k, ...\rangle = \sqrt{n_k}\,|n_0, n_1, ..., n_k - 1, ...\rangle \\ \hat{a}_k^\dagger \,|n_0, n_1, ..., n_k, ...\rangle = \sqrt{n_k + 1}\,|n_0, n_1, ..., n_k + 1, ...\rangle \end{cases} \tag{2.7}$$

These operators follow the usual bosonic algebra:

$$\begin{cases} \left[\hat{a}_k, \hat{a}_{k'}^\dagger\right] = \delta_{kk'} \\ [\hat{a}_k, \hat{a}_{k'}] = \left[\hat{a}_k^\dagger, \hat{a}_{k'}^\dagger\right] = 0 \end{cases} \tag{2.8}$$

It could also be useful to define operators able to annihilate and create particles at a given position. Thus, we define the field operators $\hat{\psi}(\boldsymbol{r})$ and $\hat{\psi}^\dagger(\boldsymbol{r})$:

$$\hat{\psi}(\boldsymbol{r}) = \sum_{k=0}^{\infty} \langle \boldsymbol{r}|\phi_k\rangle \, \hat{a}_k \ , \ \hat{\psi}^\dagger(\boldsymbol{r}) = \sum_{k=0}^{\infty} \langle \phi_k|\boldsymbol{r}\rangle \, \hat{a}_k^\dagger \tag{2.9}$$

These operators also follow a typical bosonic algebra:

$$\left[\hat{\psi}(\boldsymbol{r}), \hat{\psi}^\dagger(\boldsymbol{r})\right] = \delta(\boldsymbol{r} - \boldsymbol{r'}) \tag{2.10}$$

Those operators will be of great use to simplify computations. Indeed, such quantized fields are equivalent to our many-body system i.e. all the information about our system is contained in those field operators [47]. To conclude this section, one should notice that observables can be expressed in terms of $\hat{\psi}(\boldsymbol{r})$ and $\hat{\psi}^\dagger(\boldsymbol{r})$:

$$\text{One-body observable: } \hat{M} = \int_{\mathbb{R}^3} d\boldsymbol{r} \ \hat{\psi}^\dagger(\boldsymbol{r}) M(\boldsymbol{r}) \hat{\psi}(\boldsymbol{r}) \tag{2.11}$$

$$\text{Two-body observable: } \hat{M} = \frac{1}{2} \int_{\mathbb{R}^3} d\boldsymbol{r} \int_{\mathbb{R}^3} d\boldsymbol{r'} \hat{\psi}^\dagger(\boldsymbol{r}) \hat{\psi}^\dagger(\boldsymbol{r'}) M(\boldsymbol{r}, \boldsymbol{r'}) \hat{\psi}(\boldsymbol{r'}) \hat{\psi}(\boldsymbol{r}) \tag{2.12}$$

2.2 Description of a BEC

2.2.1 One-body density matrix and the Penrose-Onsager criterion

We are now able to describe a system of N scalar bosons. However we still lack a definition of Bose-Einstein condensation in that formalism as well as a criterion to determine if the system has condensed. Let us define the one-body density matrix:

$$n^{(1)}(\boldsymbol{r}, \boldsymbol{r'}) = \langle \hat{\psi}^\dagger(\boldsymbol{r}) \hat{\psi}(\boldsymbol{r'}) \rangle \tag{2.13}$$

It is easily shown using (2.9) that one can rewrite this hermitian matrix as:

$$n^{(1)}(\boldsymbol{r}, \boldsymbol{r'}) = \sum_k n_k \phi_k^*(\boldsymbol{r}) \phi_k(\boldsymbol{r'}) \tag{2.14}$$

where n_k is the occupation number of the state $|\phi_k\rangle$. It is important to emphasise that the set of vectors $|\phi_k\rangle$ are in fact the eigenstates of the one-body density matrix. The discussion here is highly formal and this formalism can be applied to non-interacting, interacting and even trapped particles [48]. Given this density matrix, we are now able to give a proper definition of BEC in the many-body formalism. A BEC is characterised by the occupation of one of the eigenstates of $n^{(1)}(\boldsymbol{r}, \boldsymbol{r'})$ by a macroscopic number of particles. Thus, a natural criterion to characterise the condensation, introduced by Penrose and Onsager [49], is that a BEC will occur if:

$$\lim_{N\to\infty} \frac{\sup_k n_k}{N} > 0 \tag{2.15}$$

This limit will give us the fraction of condensed particles N_0/N, where the index 0 refers to the macroscopically occupied state. Experimentally, a Bose-Einstein condensate will be characterised by a peak of density at low momentum as can be seen in Figure 2.1.

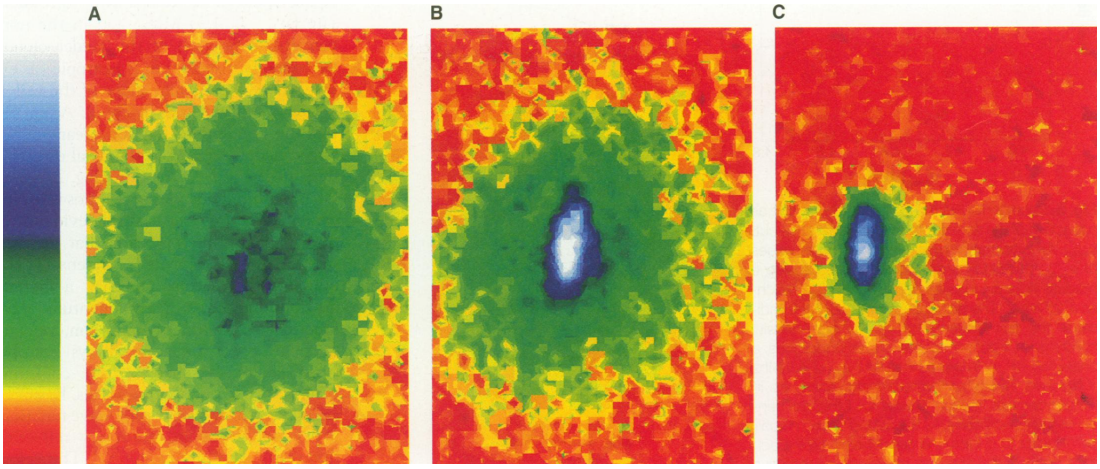

Figure 2.1: The 2D velocity distribution observed by Anderson and al. in 1995. The colour scale refers to the density for a given velocity. A bluer color indicates a larger density. On the left, the critical temperature was not reached yet. On the right, the condensation had happened and a peak may be observed for a quasi-null velocity [45].

2.2.2 The Hartree-Fock approximation

The next step to investigate our many-body system of N bosons and its condensation is the Hartree-Fock approximation. We will postulate that each boson is in the one-body eigenstate ϕ_0. In practice this means that the wavefunction of the system is given by the product of N one-body wavefunctions. Given the fact that we want to find the ground state of our system, it is wise to choose those one-body states to be the ground states of N one-body Hamiltonian. We have:

$$|\Psi_0\rangle_N = |N, 0, 0, ...\rangle \tag{2.16}$$

To keep the notation simple, we will drop the N index for the fundamental state. The field operators needed to create and annihilate particles in the ground state are easily derived from (2.9):

$$\hat{\psi}_0 = \phi_0(\boldsymbol{r})\hat{a}_0 \ , \ \hat{\psi}_0^\dagger = \phi_0^*(\boldsymbol{r})\hat{a}_0^\dagger \tag{2.17}$$

Considering a many-body Hamiltonian composed of a kinetic term, an interaction term and an external potential:

$$H = \sum_{i=1}^{N} -\frac{1}{2m}\frac{\partial^2}{\partial \boldsymbol{r_i}^2} + V(\boldsymbol{r_i}) + \frac{1}{2}\sum_{i,j=1}^{N} U(\boldsymbol{r_i} - \boldsymbol{r_j}) \tag{2.18}$$

one can rewrite this Hamiltonian as prescribed by (2.11) and (2.12):

$$\begin{aligned}\hat{H} = &\int_{\mathbb{R}^3} \hat{\psi}_0^\dagger(\boldsymbol{r}) \left(-\frac{1}{2m}\frac{\partial^2}{\partial \boldsymbol{r}^2} + V(\boldsymbol{r})\right) \hat{\psi}_0(\boldsymbol{r}) \ d\boldsymbol{r} \\ &+ \frac{1}{2}\iint_{\mathbb{R}^3} \hat{\psi}_0^\dagger(\boldsymbol{r})\hat{\psi}_0^\dagger(\boldsymbol{r'})U(\boldsymbol{r} - \boldsymbol{r'})\hat{\psi}_0(\boldsymbol{r'})\hat{\psi}_0(\boldsymbol{r}) \ d\boldsymbol{r}d\boldsymbol{r'}\end{aligned} \tag{2.19}$$

We now define the energy of the ground state as $E_0 \equiv \langle\Psi_0|\, \hat{H}\, |\Psi_0\rangle$. Using the commutation relation of the field operators leads to the following functional for E_0:

$$E_0 = N \int_{\mathbb{R}^3} \phi_0^*(\boldsymbol{r}) \left(-\frac{1}{2m} \frac{\partial^2}{\partial \boldsymbol{r}^2} + V(\boldsymbol{r}) \right) \phi_0(\boldsymbol{r}) \, d\boldsymbol{r} + \frac{N(N-1)}{2} \iint_{\mathbb{R}^3} U(\boldsymbol{r} - \boldsymbol{r'}) |\phi_0(\boldsymbol{r})|^2 |\phi_0(\boldsymbol{r'})|^2 \, d\boldsymbol{r} d\boldsymbol{r'} \tag{2.20}$$

To find the energy ground state, one minimises the above functional. Employing the Lagrange multipliers technique to ensure the correct normalisation of ϕ_0 , we are led to take the functional derivative of $E_0 - N\mu \left(\int d\boldsymbol{r} |\phi_0(\boldsymbol{r}|^2 - 1 \right)$ with respect to $\phi_0^*(\boldsymbol{r})$ rather than simply the functional derivative of E_0. One should also notice that, as is usually the case in QFT, the function $\phi_0^*(\boldsymbol{r})$ should be treated as a complex scalar field independent of $\phi_0(\boldsymbol{r})$. Therefore we obtain:

$$\frac{\delta E_0}{\delta \phi_0^*} = N \left(\frac{1}{2m} \frac{\partial^2}{\partial \boldsymbol{r}^2} + V(\boldsymbol{r}) - \mu + (N-1) \int_{\mathbb{R}^3} U(\boldsymbol{r} - \boldsymbol{r'}) |\phi_0(\boldsymbol{r'}|^2 \, d\boldsymbol{r'} \right) \phi_0(\boldsymbol{r}) = 0 \tag{2.21}$$

One can wonder about the physical significance of μ. In the limit $N \gg 1$, it is easy to check that:

$$\frac{dE_0}{dN} = \mu \iff dE = \mu dN \tag{2.22}$$

Hence μ can be interpreted as the chemical potential of our bosonic system.

2.2.3 The Gross-Pitaevskii equation

Since we work at large N, we can safely make the approximation $N - 1 \sim N$. Moreover, we will limit our investigations to ultra-cold clouds of particles. Working at very low temperature allow us to replace our two-body interaction term by the Fermi-Huang pseudo-potential [50]:

$$U_{new} = g \frac{\partial}{\partial |\boldsymbol{r} - \boldsymbol{r'}|} \delta(\boldsymbol{r} - \boldsymbol{r'}) \tag{2.23}$$

where the constant g is related to the scattering of two particles. The value of g will be crucial to study the feasibility of a BEC of axions and we shall discuss it later in this work. Injecting this potential in (2.23) leads to the following equation:

$$\left(\frac{1}{2m} \frac{\partial^2}{\partial \boldsymbol{r}^2} + V(\boldsymbol{r}) + Ng |\phi_0(\boldsymbol{r})|^2 \right) \phi_0(\boldsymbol{r}) = \mu \phi_0(\boldsymbol{r}) \tag{2.24}$$

Thereafter one can redefine the wavefunction of the BEC, Ψ_0, in such a way that the integral $\int |\Psi_0(\boldsymbol{r})|^2 d\boldsymbol{r}$ returns us the number of particles in our BEC:

$$\Psi_0(\boldsymbol{r}) = \sqrt{N} \phi_0(\boldsymbol{r}) \tag{2.25}$$

Rewriting (2.24 with this definition, one obtains the Gross-Pitaevski equation, which can be seen as a non-linear Schrödinger equation:

$$\left(\frac{1}{2m} \frac{\partial^2}{\partial \boldsymbol{r}^2} + V(\boldsymbol{r}) + g |\Psi_0(\boldsymbol{r})|^2 \right) \Psi_0(\boldsymbol{r}) = \mu \Psi_0(\boldsymbol{r}) \tag{2.26}$$

If the condensate is trapped in an external potential well, one can make a further approximation, called the Thomas-Fermi approximation (TF), consisting in neglecting the kinetic energy of the BEC. Therefore one can approximate the Gross-Pitaevskii equation by:

$$V(\boldsymbol{r}) + g|\Psi_0(\boldsymbol{r})|^2 = \mu \Longleftrightarrow \Psi_0(\boldsymbol{r}) = \sqrt{\frac{1}{g}\left(\mu - V(\boldsymbol{r})\right)} \tag{2.27}$$

This expression will allow us to compute the wavefunction of our BEC for a given trapping potential in the next chapter. However those solutions will be static ones and we shall refine our analysis to take into account the kinetic term of the Gross-Pitaevskii equation as well as an hypothetical and non-trivial time dependence of the wavefunction. The Thomas-Fermi approximation will hold as long as the length scales associated to the BEC are larger than its healing length that we define as $\xi = \sqrt{\frac{\hbar^2}{2m_a\mu}}$. The healing length may be seen as a comparison between the kinetic energy and the chemical potential. For the Thomas-Fermi approximation to hold, we require that the healing length should be small compared to other length scales of the system.

2.3 Collective excitation in BEC

When the bosonic particles composing the BEC interact, i.e. when the constant g defining the potential in (2.23) takes a non-zero value, collective behaviours may appear in a condensate subjected to a perturbation. This perturbation may give rise to a wide range of phenomena such as phonons, vortices, long-range interactions and superfluidity. To analyse their possible observational consequences, one has to introduce the Bogoliubov-de Gennes equations.

2.3.1 The Bogoliubov-de Gennes equations

Let us take Ψ_0 as solution of the Gross-Pitaevskii equation and add to it a small perturbation $\delta\Psi$ such that we can write down the wave-function of our BEC as

$$\Psi(\boldsymbol{r}, t) = \left(\Psi_0(\boldsymbol{r}) + \delta\Psi(\boldsymbol{r}, t)\right) e^{-i\frac{\mu}{\hbar}t} \tag{2.28}$$

Ψ will be our new ground state. Note that we dropped the null-index to avoid the confusion with the solution of the non-perturbed Gross-Pitaevskii equation. Now, we inject the wavefunction (2.28) in the equation (2.26). Keeping the terms of first order in $\delta\Psi$, one obtains the following equation

$$i\hbar\frac{\partial}{\partial t}\delta\Psi = \left[-\frac{1}{2m_a}\Delta + V(\boldsymbol{r}) - \mu + 2g|\Psi_0|^2\right]\delta\Psi + g\Psi_0^2\ \delta\Psi^* \tag{2.29}$$

To solve and gain some physical insights about this equation, one should now apply a Fourier transform from time to angular frequency to the perturbation

$$\delta\Psi(\boldsymbol{r}, t) = \frac{1}{2\pi}\int_0^\infty u_\omega(\boldsymbol{r})e^{-i\omega t} + v_\omega^*(\boldsymbol{r})e^{i\omega t}\ d\omega \tag{2.30}$$

This allows us to rewrite (2.29) as a system of two coupled differential equations, the Bogoliubov-de Gennes equations.

$$\begin{cases} \left[-\frac{\hbar^2}{2m_a}\Delta + V(\boldsymbol{r}) - \mu + 2g|\Psi_0|^2\right] u_\omega(\boldsymbol{r}) + g\left(\Psi_0\right)^2 v_\omega(\boldsymbol{r}) = \omega u_\omega(\boldsymbol{r}) \\ \left[-\frac{\hbar^2}{2m_a}\Delta + V(\boldsymbol{r}) - \mu + 2g|\Psi_0|^2\right] v_\omega(\boldsymbol{r}) + g\left(\Psi_0^*\right)^2 u_\omega(\boldsymbol{r}) = -\omega v_\omega(\boldsymbol{r}) \end{cases} \tag{2.31}$$

Unfortunately, those equations are usually not solvable and one has to use numerical tools to obtain the functions $u_\omega(\boldsymbol{r})$ and $v_\omega(\boldsymbol{r})$. We will not try to solve the Bogoliubov-de Gennes equations in this work since it would require much supplementary work for a Master thesis. However, we wanted to introduce them due to their potential utility for explaining such phenomena as the long range interaction discussed by Berezhiani [51]. We are now well equipped to study the Bose-Einstein condensation of axions and others ALPs.

3

BEC of axions

3.1 Axions and ALP self-interaction

3.1.1 Some QFT reminders

As mentioned in section 2.2.3, the interaction between our constituting particles is decisive to the Bose-Einstein condensation. The axion-axion interaction is usually treated as a triviality in the literature. Most authors neglect it in the first stage of their development [51, 52]. However, one has to take into account that such light scalar particles possess Compton wavelength reaching parsecs in length. Hence the interaction cannot be treated as a short-distance scattering as is usually the case. We shall thus compute the cross-section of axion-axion scattering properly to extract the g constant that describes the two-body interaction in (2.26). To do so, some scattering theory basics in the QFT formalism could be useful and we should thus begin this section by a brief reminder of the topic.

Free scalar field

Since the axion is a scalar field, we will take for our discussion a general free scalar field described by the action

$$S\left[\phi\right] = \int \mathcal{L}\ d^4x \tag{3.1}$$

where the Lagrangian density $\mathcal{L}$ takes the form

$$\mathcal{L} = -\frac{1}{2}\partial_\mu\phi\partial^\mu\phi - \frac{m}{2}\phi^2 \tag{3.2}$$

Taking the extremum of this action leads us to the usual Klein-Gordon equation

$$\left(\Box + m^2\right)\phi = 0 \tag{3.3}$$

and we thus have the general solution

$$\phi(t) = \int \frac{d^3p}{(2\pi)^3}\frac{1}{\sqrt{2p_0}}\left(a_p e^{ip_\mu x^\mu} + a_p^* e^{-ip_\mu x^\mu}\right) \tag{3.4}$$

where we should not worry too much about the $\frac{1}{\sqrt{2p_0}}$ factor, present to ensure relativistic normalisation. Applying second quantization to our scalar field promotes $\phi(t)$ to $\hat{\phi}(t)$ and

the coefficient a_p and a_p^* also become operators assuming roles similar to that of the the operators introduced in equation (2.7). Thus, the operator $\hat{\phi}^\dagger(x)$ applied to the vacuum state $|0\rangle$ creates a scalar particle at a point x in space-time while the operator $\hat{\phi}(x)$ annihilates one. The free field theory is quite simple. However our goal is to describe interaction between the scalar field and itself and we should introduce a term to our Lagrangian density to describe this interaction. Nevertheless it will prove more difficult than it may seem at first glance and one should introduce the interaction picture before looking at the problem.

The different pictures of Quantum Mechanics

We have two objects in a quantum theory: a Hilbert space where the quantum state describing our system lives and the set of operators that can act on this Hilbert space. Choosing a picture consists in choosing between the operators and the vector states which will carry the time dependence and we can define three main pictures.

- The Schrödinger picture places the time dependence on the quantum state and the time evolution of this state is given by

$$|\psi(t)\rangle = \hat{U}(t, t_0)\,|\psi(t_0)\rangle = e^{-i\hat{H}(t-t_0)}\,|\psi(t_0)\rangle \tag{3.5}$$

- The Heisenberg picture places the time dependence on the operators while keeping the vector space frozen in time. The time evolution of an operator $\hat{M}$ is given by

$$\frac{d\hat{M}}{dt} = i\left[\hat{H}, \hat{M}\right] + \frac{\partial \hat{M}}{\partial t} \tag{3.6}$$

- The interaction or Dirac picture takes a hybrid position and is a little more subtle. The idea is to decompose the Schrödinger Hamiltonian appearing in (3.5) into two parts

$$\hat{H} = \hat{H}_0 + \hat{H}_I \tag{3.7}$$

  where $\hat{H}_0$ is well known (the Hamiltonian for the theory without interaction) and $\hat{H}_I$ is a perturbation to the free Hamiltonian due to interaction with other fields. This perturbative Hamiltonian will be accountable for the time evolution of the Hilbert space

$$|\psi(t)\rangle = e^{-i\hat{H}_I t}\,|\psi(0)\rangle \tag{3.8}$$

  while the operators will be evolving as they were in the free theory described by $\hat{H}_0$

$$\frac{d\hat{M}}{dt} = i\left[\hat{H}_0, \hat{M}\right] + \frac{\partial \hat{M}}{\partial t} \tag{3.9}$$

While these pictures seem mathematically equivalent and related by unitary transformations, we could discuss the physical significance of those different representations and what they tell us about the nature of vector states and observables then leading us to more fundamental questions about the content of a vector state or the meaning of a measurement. However, we will restrict ourselves to choosing a picture according to its technical usefulness. It happens that in the case of a quantum field theory, it will be easier to use the interaction picture.

The interaction Hamiltonian and the S matrix

From the Lagrangian for our free scalar field, we have seen that it is easy to compute the equations of motion for the field. Alternatively, one could have derived the equations governing the field thanks to the Hamiltonian corresponding to the free theory. Now, one should find the self-interaction Hamiltonian for a scalar field. The interaction Lagrangian density is given by [35]

$$\mathcal{L}_I = -\frac{\lambda}{4!}\phi^4 \tag{3.10}$$

where the λ parameter describe the strength of the self-interaction. Since this Lagrangian is not a function of the conjugated momenta, one obtain for the interaction Hamiltonian density

$$\mathcal{H}_I = -\mathcal{L}_I = \frac{\lambda}{4!}\phi^4 \tag{3.11}$$

We should then study the evolution of a quantum state under the action of $\mathcal{H}_I$. Let us look at a state in the distant past, governed by the free Hamiltonian.

$$|\Psi(t=-\infty)\rangle = |i\rangle \tag{3.12}$$

We then define a matrix S such that the free state in a far future is given by

$$|\Psi(t=+\infty)\rangle = S\,|i\rangle = \sum_f S_{fi}\,|i\rangle \tag{3.13}$$

We next have to find a link between the Hamiltonian and the S matrix. From (3.8), one has the Schrödinger equation

$$i\frac{d}{dt}\,|\Psi(t)\rangle = \hat{H}_I\,|\Psi(t)\rangle \tag{3.14}$$

where $\hat{H}_I$ is the Hamiltonian associated to the Hamiltonian density (3.11). One can use a perturbative approach to rewrite this equation. At the first order one obtains

$$\begin{aligned} |\Psi(t)\rangle &= |i\rangle + \int_{-\infty}^{t} dt_1 \frac{H_I(t_1)}{i}\,|\Psi(t_1)\rangle \\ &= |i\rangle + \int_{-\infty}^{t} dt_1 \frac{H_I(t_1)}{i}\,|i\rangle + \int_{-\infty}^{t} dt_1 \int_{-\infty}^{t_1} dt_2 \frac{H_I(t_1)}{i}\frac{H_I(t_2}{i}\,|\Psi(t_2)\rangle \\ &\vdots \end{aligned} \tag{3.15}$$

And thus one can write the state in a faraway future as

$$|\Psi(t=+\infty)\rangle = \sum_{n=0}^{\infty} \frac{1}{i^n} \int_{-\infty}^{+\infty} dt_1 \int_{-\infty}^{t_1} dt_2 \ldots \int_{-\infty}^{t_{n-1}} dt_n H_I(t_1)\ldots H_I(t_n)\,|i\rangle \tag{3.16}$$

One can compare this equation to (3.13) and re-express the integral boundaries. Moreover, one can use the definition

$$H_I(t) = \int d^3x \mathcal{H}_I(t) \tag{3.17}$$

to write the S matrix as

$$S = \sum_{n=0}^{\infty} \frac{(-i)^n}{n!} \int d^4x_1 \dots \int d^4x_n \; T\left(\mathcal{H}_i(t_1) \dots \mathcal{H}_i(t_n)\right) \tag{3.18}$$

with T the time-ordering operator such that

$$T\left(f(t_1)f(t_2)\right) = \begin{cases} f(t_1)f(t_2) & \text{if} \quad t_1 > t_2 \\ \\ f(t_2)f(t_1) & \text{if} \quad t_2 > t_1 \end{cases} \tag{3.19}$$

Since the self-interaction parameter λ is extremely small for the axion field, one can keep only the first order terms in (3.18). One obtains

$$S = 1 - iT\left(\int d^4x \; \mathcal{H}_I(t_1)\right) = 1 - iT\left(\frac{\lambda}{4!}\int d^4x \; \phi^4\right) \tag{3.20}$$

Elements of the S matrix and cross-section

Given the approximate expression obtained for the S-matrix, one can compute its elements for free particles in the initial and final states. We are interested by axion-axion scattering ($aa \to aa$) and we will thus study the following case: two particles of momenta $\boldsymbol{k_1}$ and $\boldsymbol{k_2}$ in this initial state giving two particles with momenta $\boldsymbol{p_1}$ and $\boldsymbol{p_1}$ in the final state. Thanks to the creation operators defined earlier, it is easy to write those states as

$$\begin{aligned} |\boldsymbol{k_1 k_2}\rangle &= 2\sqrt{E_{\boldsymbol{k_1}} E_{\boldsymbol{k_2}}} a^\dagger_{\boldsymbol{k_1}} a^\dagger_{\boldsymbol{k_2}} |0\rangle \\ |\boldsymbol{p_1 p_2}\rangle &= 2\sqrt{E_{\boldsymbol{p_1}} E_{\boldsymbol{p_2}}} a^\dagger_{\boldsymbol{p_1}} a^\dagger_{\boldsymbol{p_2}} |0\rangle \end{aligned} \tag{3.21}$$

where the prefactors ensure relativistic normalisation of our states. Hence we can try to compute the S-matrix elements. The first term due to the identity matrix leads to

$$\langle \boldsymbol{p_1 p_2} | \boldsymbol{k_1 k_2} \rangle = 4E_{\boldsymbol{k_1}} E_{\boldsymbol{k_2}} (2\pi)^6 \left(\delta^{(3)}(\boldsymbol{p_1} - \boldsymbol{k_1})\delta^{(3)}(\boldsymbol{p_2} - \boldsymbol{k_2}) + \delta^{(3)}(\boldsymbol{p_1} - \boldsymbol{k_2})\delta^{(3)}(\boldsymbol{p_2} - \boldsymbol{k_1})\right) \tag{3.22}$$

Obviously this matrix element does not really contribute to scattering and corresponds to the case where our particles do not interact. The interesting part lies in the term involving our interaction Hamiltonian. This element reads

$$\langle \boldsymbol{p_1 p_2}| - iT\left(\frac{\lambda}{4!}\int d^4x \; \phi^4\right) |\boldsymbol{k_1 k_2}\rangle \tag{3.23}$$

Due to the presence of the time-ordering operator, it may seem difficult to compute such a matrix element. Fortunately enough one may use here the Wick theorem to simplify this expression. Wick's theorem states that the time-ordered product of operators can be expressed as the sum of normal-ordered field operator and Feynman propagators. The Feynman propagator, which is a specific Green's function, takes a particle in a space-time event x_1 and brings it to the event x_2. We will use the following notation

$$D_F(x_1 - x_2) \equiv \overbrace{\phi_1 \phi_2} \tag{3.24}$$

For four fields, as we will need for our Hamiltonian, Wick's theorem reads

$$T\left(\phi_1\phi_2\phi_3\phi_4\right) = N\Big(\phi_1\phi_2\phi_3\phi_4 + \overbrace{\phi_1\phi_2}\phi_3\phi_4 + \overbrace{\phi_1\phi_2\phi_3}\phi_4 + \overbrace{\phi_1\phi_2\phi_3\phi_4} + \phi_1\overbrace{\phi_2\phi_3}\phi_4 + \phi_1\overbrace{\phi_2\phi_3\phi_4} + \phi_1\phi_2\overbrace{\phi_3\phi_4} + \overbrace{\phi_1\phi_2}\overbrace{\phi_3\phi_4} + \overbrace{\phi_1\overbrace{\phi_2\phi_3}\phi_4} + \overbrace{\phi_1\overbrace{\phi_2\phi_3\phi_4}}\Big) \tag{3.25}$$

It can be shown [35] that the only term contributing to the scattering is the first term. We are thus left with four field operators. Two of them should be applied to annihilate the two incoming particles and two should recreate them with the right momenta in the final state. However, due to the symmetry of the Hamiltonian with respect to the permutation of the four field operators, we are led to the following expression

$$\begin{aligned}\langle \boldsymbol{p_1 p_2}| - iT\left(\frac{\lambda}{4!}\int d^4x\ \phi^4\right)|\boldsymbol{k_1 k_2}\rangle &= 4!\left(-i\frac{\lambda}{4!}\right)\int d^4x e^{-i(k_1+k_2-p_1-p_2)_\mu x^\mu} \\ &= -i\lambda(2\pi)^4\delta^{(4)}(k_1+k_2-p_1-p_2)\end{aligned} \tag{3.26}$$

Reinserting this matrix element into the expression for the cross-section of two-body scattering in the center-of-mass frame and integrating over the Lorentz-invariant phase space finally give

$$\sigma = \frac{\lambda^2}{32\pi E_{cm}^2} \tag{3.27}$$

where E_{cm}^2 is the energy in the center of mass.

3.1.2 S-Wave scattering length and self-interaction

At low temperature, the only relevant parameter for the scattering is the s-wave scattering length, the value of which is given by

$$a_s = \lim_{\boldsymbol{p},\boldsymbol{k}\to 0}\sqrt{\frac{\sigma}{4\pi}} = \frac{\lambda}{16\pi m_a} \tag{3.28}$$

The relation between the s-wave scattering length and the constant g of chapter 2 defining our two-body interaction may be derived from scattering theory [53]

$$g = \frac{4\pi a_s}{m_a} = \frac{\lambda}{4m_a^2} \tag{3.29}$$

The s-wave scattering length can be positive or negative. Negative values of this parameter are associated with an attractive interaction while the positive values correspond to a repulsive interaction between particles. Taking a postive value of a_s thus ensures a positive value of the lambda parameter. Having a repulsive self-interaction ($\lambda > 0$) allows us to have a stable vacuum. For negative values of λ, one obtains an attractive interaction. However, this attractive interaction leads to a metastable vacuum. This is the case for the QCD axion. For a very narrow range of values, QCD axions and self-attractive ALPs can form small metastable condensates called Bose stars. These stars, comparable to black holes or neutron stars in term of density and size, could theoretically account for a part

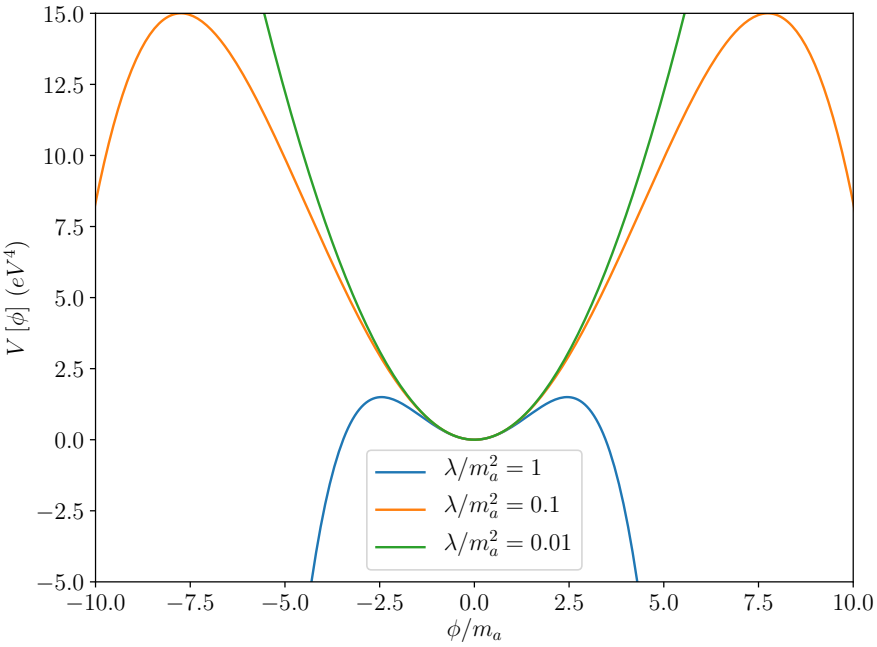

Figure 3.1: The potential $V[\phi]$ for different values of the ratio λ/m_a^2.

of dark matter [54]. We shall now discuss the problem of the metastable vacuum. We can give an intuitive argument by looking at the potential appearing in the Lagrangian to see that an attractive interaction is viable in that case. On the figure 3.1, we can clearly see that the vacuum of the theory at $|\phi|/m_a = 0$ is metastable and that it could cause some issue even at low energy. However, if the self-interaction constant λ becomes small enough compared to the mass, the vacuum of our theory becomes more stable. We can thus safely work with an attractive self-interaction for our scalar field without fearing disasters to occur. To show that the model is coherent, it is of interest to derive the half-life of our Universe as a function of m_a and λ for such a false vacuum. It is important here to understand that this argument only gives a hint of how and why attractive scalar fields may be viable. Rigorous treatment of the matter is highly non-trivial and the topic is still open to discussion [55].

Lifetime of the Universe

It is possible for a purely classical field to possess two stable vacua. Once the system reaches one of those vacua, it remains there forever. However, this is not the case for a quantum theory. Indeed, if the field reaches a false vacuum, i.e. a local vacuum of higher energy than the true vacuum, it can tunnel through the potential barrier. One may imagine this phenomenon as beautifully explained by Sidney Coleman in [56]. The transition between the two vacua can be compared to a nucleation process. We take an expanding universe endowed with our scalar field. Due to quantum fluctuations, bubbles of absolute vacuum may appear. However, if the bubble is small enough, its creation is not energetically favourable. Nevertheless, one could imagine a bubble large enough to be energetically favourable which would then expand and convert the false vacuum into the true vacuum, leading to the annihilation of stars, galaxies and others structures. Since all those types of structures are still observed today, our model should predict a lifetime

for the Universe large enough. In fact, the important factor here is the probability of transition per unit of time and volume, Γ/V. To find the predicted age of the Universe, we would like to find the cosmic time t for which the four-volume of the past light-cone multiplied by the ratio Γ/V is equal to one. If the time obtained is larger than the present cosmic time by multiple orders of magnitude, we could then safely assume that the vacuum of the theory is stable enough. Γ/V can be expressed as [56]

$$\Gamma/V = Ae^{-B} \tag{3.30}$$

Our duty is thus to determine the two parameters A and B as functions of m_a and λ. We now derive the B parameter following the procedure described in [56]. To do so, we first need to use a special trick. Our potential is given by

$$V_{[}\phi] = \frac{m_a^2}{2}\phi^2 + \frac{\lambda}{4!}\phi^4 \tag{3.31}$$

Technically, the vacuum can only be defined at $\phi = 0$ since this potential has no global minimum (for a negative value of λ). However, we need two vacua to apply the formalism developed by Coleman. We will thus assume that the field would tunnel to a state of smaller energy with a difference ϵ between the original vacuum and the final state located at $\phi = l = \sqrt{\frac{12m_a^2}{\lambda}}$. We now have to compute

$$S = \int_0^l \sqrt{2V[\phi]}\; d\phi = \int_0^l \sqrt{m_a^2\phi^2 + \frac{\lambda}{12}\phi^4}\; d\phi \tag{3.32}$$

Choosing $m_a = 10^{-20}$ and $\lambda = 10^{-40}$, which are reasonable values considering our hypotheses, we get $S = 4\,10^{-20}$. We will use this value to obtain an estimation of the life-time predicted for our universe. According to Coleman, the B coefficient is given by

$$B = 27\pi^2\frac{S^4}{2\epsilon^3} \tag{3.33}$$

with the condition that ϵ be small compared to the natural scale m_a^4/λ of our field

$$\frac{m_a^4}{\lambda\epsilon} >> 1 \tag{3.34}$$

The theory behind the A parameter is somewhat more technical and implies Feynman's sum over histories as well as complex analysis computation beyond the scope of this work. Nevertheless, [57] gives us an expression for A and we thus reach the following

$$\Gamma/V \approx \frac{B^2}{4\pi^2}e^{-B}\ \mathrm{eV}^4 \tag{3.35}$$

The last step of the calculation consists in finding the four-volume of the past light-cone. The expression for this volume obviously varies as a function of the metric tensor. We have

$$\mathcal{V} = \int_{\mathcal{C}} \sqrt{-g}\; d^4x \tag{3.36}$$

where $\mathcal{C}$ describes our light cone and is still to be determined. For the FLRW metric expressed in conformal time and spatial spherical coordinates

$$ds^2 = a^2(\eta)\left(-d^2\eta + d^2r + r^2d^2\theta + r^2\sin^2\theta d^2\phi\right) \tag{3.37}$$

one can easily find the null-geodesic equation for purely radial geodesics

$$d\eta = \pm dr \tag{3.38}$$

Once this equation obtained, we can finally write the following expression

$$\mathcal{V} = \int_0^{2\pi} \int_0^{\pi} \int_0^{\eta_0} \int_{-\eta}^{\eta} a^4(\eta) r^2 \sin\theta d\theta d\phi d\eta dr \tag{3.39}$$

which leads, after integration, to

$$\mathcal{V} = \frac{8\pi}{3} \int_0^{\eta_0} a^4(\eta) \eta^3 \, d\eta \tag{3.40}$$

The last unknown of our derivation is the scale factor $a(\eta)$, needed to find the four-volume as well as the conformal time. It obviously varies as a function of the content of the Universe. Since we have the following definition for the conformal time elapsed since the Big Bang

$$\eta = \int_0^t \frac{dt}{a(t)} \tag{3.41}$$

one can easily find the expression of $a(\eta)$ for a given $a(t)$. For instance, in the case of a radiation-dominated universe one has $a(t) = \sqrt{t}$ thus leading to $a(\eta) = \eta/2$ with $\eta \in [0, +\infty]$. For such a universe one would get a four-volume

$$\mathcal{V} = \frac{\pi}{48} \eta_0^8 \tag{3.42}$$

We should now solve the following equation

$$\frac{B^2 \eta_0^8}{192\pi} e^{-B} = 1 \tag{3.43}$$

Thus we have

$$\eta_0 = \left(\frac{192\pi}{B^2} e^B \right)^{1/8} \tag{3.44}$$

We see here that we have a competition between the prefactor that tends to diminish the conformal time and the age of the universe and the exponential which tends to increase this age. To compute a numerical value, we should fix the value of ϵ. Looking at the worst scenario where $m_a^4/\lambda\epsilon \approx 1$ i.e. $\epsilon \approx 10^{-40}$, we obtain

$$t \approx \frac{\eta_0^2}{4} = 1.63\, 10^{-11} \left(e^{8.5\, 10^{43} \pi^2} \right)^{1/8} \ \text{eV}^{-1} \tag{3.45}$$

This time is far greater than the current age of the universe by multiple orders of magnitude and the model does not contradict the observation at this point. We have neglected multiple factors during this analysis. We applied the tunnelling theory without the existence of a second vacuum and we did not take into account other interactions. A more comprehensive discussion of the problem, including the effects of gravity on vacuum decay may be found in [58]. Nevertheless this computation endows us with a first approximation and fainter effects should not modify the qualitative results. One can thus imagine ALPs or QCD axions with an attractive interaction forming small BEC. We will not try

to discuss this kind of structures further for their number would be hard to quantify and no easy observational comparison could be made. In the next sections and chapters of this work, we will work with a positive value of λ, leading to more stable BEC that can reach galactic size, as it will be shown later.

3.1.3 Parameter space

Mass and decay constant

At this stage one could look at the values of different parameters such as m_a or λ. The parameter space is still very wide despite the fact that numerous experiments have drastically reduced the viable values for the mass and the interaction between hypothetical dark matter constituents. We cannot emphasise enough the importance of these values. On the one hand, they could discard the BEC model if they do not allow the condensation. On the other hand, they could also discard some dark matter models and thus point towards a physical origin of the axion. Suffice to say that the analysis of the parameter space is essential. We will not discuss here the different experiments neither will we discuss how various astrophysical observations allow us to constrain the parameter space. We will restrict ourselves to a review of the allowed values and their impact on a plausible BEC of axions. As is shown in Figure 3.2, axions or ALPs with a mass above 10^{-3}eV

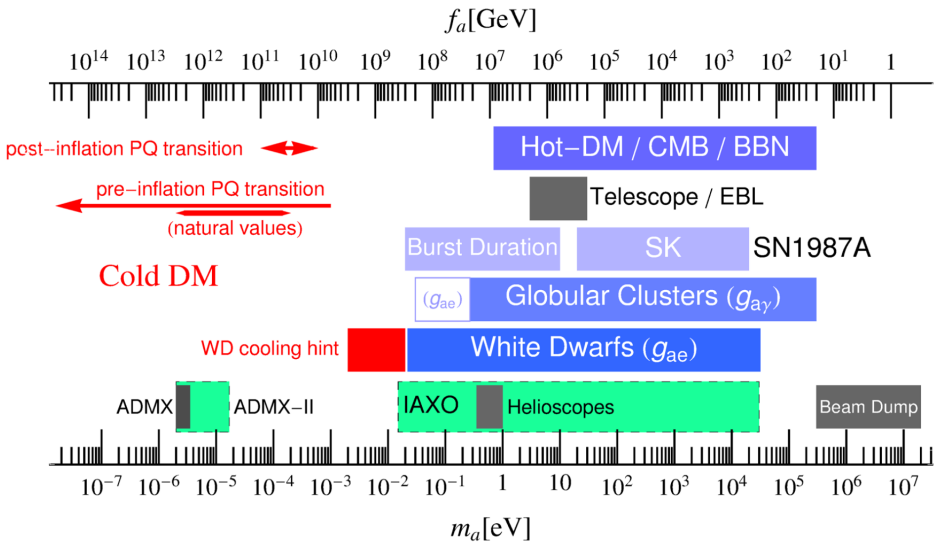

Figure 3.2: Exclusion ranges from laboratory experiments and astrophysical constraints. The grey area for the ADMX experiment corresponds to its nowadays range. The figure was taken from [59]

.

can be safely ruled out. Cold dark matter models (CDM) predict particles having a mass around 10^{-6} eV. We could also find the axions at a much lower mass scale. A serious alternative to CDM is the fuzzy dark matter (FDM), which could be composed of ultralight bosons with a mass around 10^{-22} eV [60]. Thus the possible mass covers a range of sixteen orders of magnitude. Now, one should discuss the λ parameter.

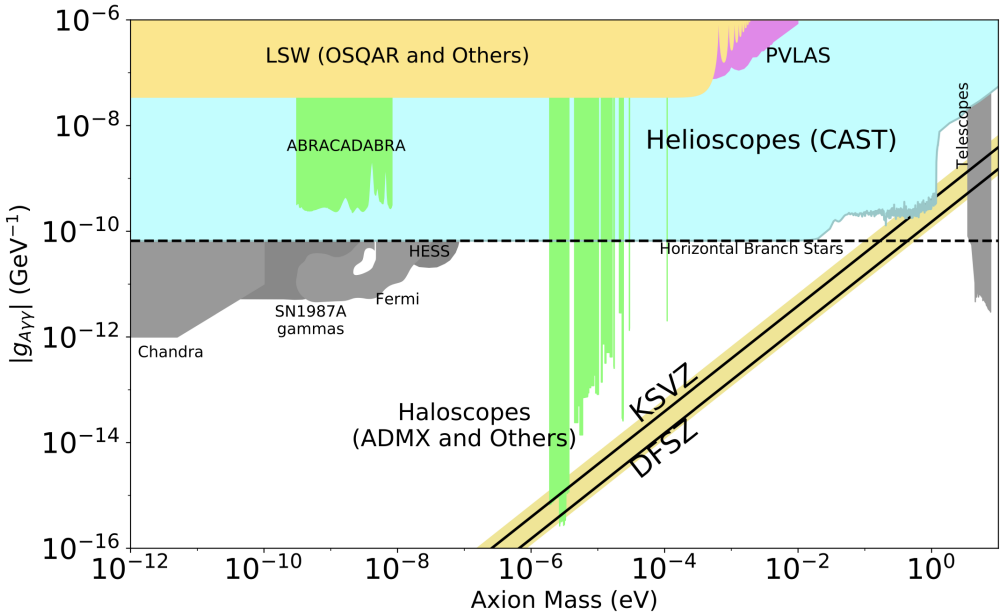

Figure 3.3: Exclusion plot for the coupling between an ALP and two photons. Figure taken from [61].

Self-interaction and Other Interactions

Axions and ALPs may interact with themselves as well as with electromagnetic fields, however weakly. Multiple astrophysical observations and experiments allow to constraint the parameter space for the λ parameter of self-interaction and for the other coupling. As mentioned above, the QCD axion is not a good candidate for our galactic condensate but the tables presented in this section are more general and concerned all ALPs. For the self-interaction parameter, no real exclusion areas exist except for the one that would lead to a metastable universe with a short lifetime. The other interactions are extremely weak and will be neglected in our simple model. Why do so while gravity is also extremely weak? Simply because gravity is a long-range interaction whereas axions interact with photons and baryons on shorter distances. However, they should be taken into account to develop more precise BEC models or verify certain predictions, especially the coupling to photon. The allowed parameter space for axion-photon coupling is shown in Figure 3.3.

3.2 Wave-function and density profile of the BEC

3.2.1 Gravitational self-trapping

The first attempt that can be made to describe a BEC is perhaps the simplest physical set-up. As mentioned earlier, the Compton wavelength of axions spreads over many parsecs. Hence the simplest case is that of an axion cloud only trapped by its own gravity. Let a cluster of N axions be in an area only subject to their own gravitational field. The ground state of the system can be described via the formalism introduced in Chapter 2. The axion BEC follows the Gross-Pitaevskii equation (2.26). Furthermore, one shall define the matter density $\rho(\boldsymbol{r}) = m_a|\Psi_0(\boldsymbol{r})|^2$. We may use a non-relativistic expression for the

gravitational potential since the masses and the momenta of our bosons are quasi-null. Working in the Thomas-Fermi approximation, which, as mentioned earlier, consists in neglecting the kinetic energy of the axions, we can describe our system by a set of two coupled differential equations:

$$\begin{cases} V(\boldsymbol{r}) + \frac{g}{m_a}\rho(\boldsymbol{r}) = \mu \\ \\ \Delta\Phi = 4\pi G\rho(\boldsymbol{r}) \end{cases} \tag{3.46}$$

Taking the Laplacian of the first equation then leads to

$$4\pi G\rho(\boldsymbol{r})m_a + \frac{g}{m_a}\Delta\rho(\boldsymbol{r}) = 0 \tag{3.47}$$

By substituting g with its expression in terms of a_s and assuming spherical symmetry, we can rewrite this equation as

$$\frac{1}{r^2}\frac{\partial}{\partial r}r^2\frac{\partial}{\partial r}\rho = -\frac{Gm_a^3}{a_s}\rho \tag{3.48}$$

Next we shall define two new variables to make our equation dimensionless

$$\theta = \rho/\rho_0 \qquad \tau = \sqrt{\frac{Gm_a^3}{a_s}}\, r \tag{3.49}$$

By injecting those two expressions in (3.48), one can rewrite it as a Lane-Emden equation [62], which is a well-studied class of equations often used in astrophysics

$$\frac{1}{\tau^2}\frac{\partial}{\partial\tau}\tau^2\frac{\partial}{\tau}\theta + \theta = 0 \tag{3.50}$$

The solution of this kind of equations is then given by a sampling function

$$\theta(\tau) = \frac{\sin\tau}{\tau} \leftrightarrow \rho(r) = \rho_0\frac{\sin\sqrt{\frac{Gm_a^3}{a_s}}\, r}{\sqrt{\frac{Gm_a^3}{a_s}}\, r} \tag{3.51}$$

Mathematically speaking, we could also have looked at other solutions implying cosines functions or an imaginary exponential. However, using a cosines instead of a sines in (3.51) leads to a divergence in the density profile at 0, which we try to avoid, and the general solution implying the imaginary exponential carries an imaginary part and cosines functions also leading to unwanted divergences. One should notice that (3.51) can also be obtained from the hydrodynamic equations describing a quantum fluid [63]. Since the density profile of the BEC has been derived, one can try to compute the radius and the total mass of the condensed cloud as functions of m_a and a_s.

BEC radius and mass

The maximum radius R_{max} is given by the first root of our function ρ since it takes negative values after it

$$R_{max} = \sqrt{\frac{a_s}{Gm_a^3}}\, \pi \tag{3.52}$$

For an axion mass of 10^{20} and a self-interaction parameter of 10^{80}, we would get a maximum radius of $\sim 10^{28}$ eV^{-1}, i.e. around 100 kpc. Is this value realistic? Yes, the galactic halo of the Milky Way for instance is some 400 kpc wide [64]. Nevertheless, if we work in the Thomas-Fermi approximation, the model provides a single radius for the dark matter cluster, which is not what one can observe. However, one should not forget that this is still a toy model and that our only constraints were the interaction between particles through gravity. It is to be expected that a single radius emerges. This computation allows us to write down the wavefunction of our BEC for a TF self-trapping potential

$$|\Psi_0(r)|^2 = \mathcal{N}\frac{\sin\sqrt{\frac{Gm_a^3}{a_s}}\,r}{\sqrt{\frac{Gm_a^3}{a_s}}\,r} \tag{3.53}$$

where $\mathcal{N}$ is a normalisation factor still to be determined. To do so, we use the fact that the integral of the probability density over the confinement space should return N for an N-body system. Using the notation $\kappa = \sqrt{\frac{Gm_a^3}{a_s}}$ to ease the reading, one finds

$$4\pi\int_0^{R_{max}} dr\ |\Psi_0|^2 r^2 = 4\pi\mathcal{N}\int_0^{\pi/\kappa} dr\frac{\sin\kappa r}{\kappa}r = \frac{4\pi^2\mathcal{N}}{\kappa^3} = N \tag{3.54}$$

Therefore, with a normalisation factor $\mathcal{N} = \frac{\kappa^3 N}{4\pi^2}$, one can link the central density of the cluster $\rho(0) = \rho_0$ to the number of axions and thus to the total mass M_{tot} of the cloud

$$\rho_0 = \frac{\kappa^3 M_{tot}}{4\pi^2} = \frac{\left(\frac{Gm_a^3}{a_s}\right)^{3/2} M_{tot}}{4\pi^2} \tag{3.55}$$

This equation can be rewritten more compactly using R_{max}

$$\rho_0 = \frac{\pi M_{tot}}{4R_{max}^3} \tag{3.56}$$

On a less technical side, one could ask whether or not we are entitled to use quantum mechanics to describe such a cloud of axions. We mean by this that, of course, the equations are solvable and the conditions to reach Bose-Einstein condensation are satisfied but can quantum physics describe a galactic-size cloud? If the question may seem a bit philosophical, we should not ignore the insights that such a question can bring to the discussion.

Chemical potential and healing length

We are now able to derive the expression of the chemical potential and of the healing length of the condensate, which will be helpful in further developments. From equation (3.46), one has

$$N = \frac{4\pi}{g}\int_0^{R_{max}} (\mu - V(\boldsymbol{r}))\ r^2 dr \tag{3.57}$$

with $V(\boldsymbol{r})$ the potential energy that we can easily compute

$$V(r) = \frac{4\pi G\rho_0 m_a}{r}\left(\frac{\sin\kappa r - \kappa r\cos\kappa r}{\kappa^3}\right) \tag{3.58}$$

$$= \frac{GM_{tot}m_a}{\pi r}\left(\sin\kappa r - \kappa r\cos\kappa r\right) \tag{3.59}$$

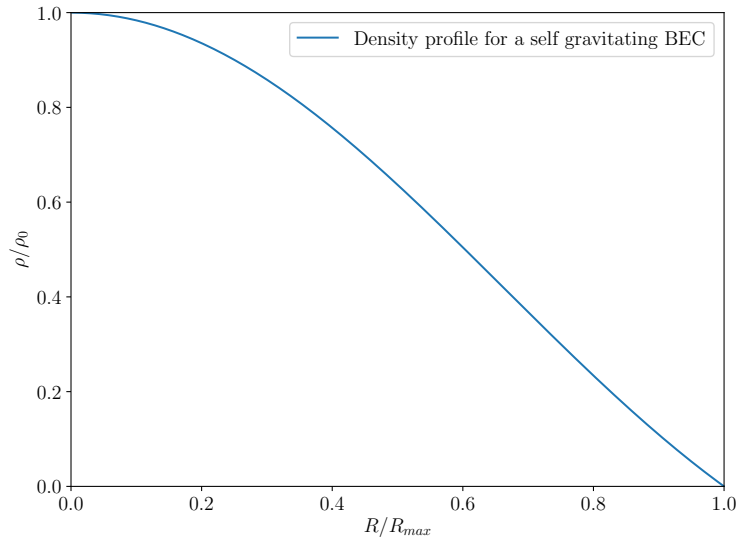

Figure 3.4: Density profile of the axion cloud in its BEC state. The axes have been normalised and made dimensionless.

We obtain the following equality

$$N = \frac{\pi}{3g} R_{max}^3 \mu \tag{3.60}$$

which can be rewritten as

$$\mu = \frac{12N}{\pi^3} \sqrt{\frac{G^3 m_a^7}{a_s}} \tag{3.61}$$

The healing length of our condensate is then given by

$$\xi = \sqrt{\frac{1}{2m_a \mu}} = \left(\frac{\pi^6 a_s}{576 N^2 G^3 m_a^9} \right)^{1/4} \tag{3.62}$$

Those different values are function of N, the number of particles in our condensate or of the total mass M_{tot}. If we take a total mass of 60 10^{10} solar masses,which equals $\sim 10^{77}$ eV, we obtain $N \approx 10^{97}$ axions in our galaxy. Equation (3.62) then leads to a healing length of 10^{22} eV^{-1} or 0.1 pc. The typical scale of our condensate here is of the order of 1 kpc. The Thomas-Fermi approximation thus holds in our case.

3.2.2 Rotating BEC

Now that we have a simple model, we can try to improve it to take into account effects such as the rotation of the axion halo. At this stage we can still work in the TF approximation and add an energy term $V_{rot}(\boldsymbol{r}) = m_a \omega^2 \boldsymbol{r}^2/2$ to take the rotation into consideration. This approach may seem naive since the angular velocity ω should realistically be a function of the radius and thus depend of the wavefunction itself. However we will consider that the BEC is slowly rotating and that ω is approximately constant. Taking the Laplacian of this term and adding it to Equation (3.47) we obtain

$$4\pi G\rho(\boldsymbol{r})m_a + \frac{g}{m_a}\Delta\rho(\boldsymbol{r}) + m_a\omega^2 = 0 \tag{3.63}$$

which can once again be rewritten as a Lane-Emden equation. By defining $\Omega = \frac{\omega^2}{2\pi G\rho}$, the solution of this equation and a derivation similar to section 3.2.1, one finds

$$R_{rot} = R_{max}\left(1+3\Omega\right)^{1/3} \qquad M_{rot}^{tot} = M_{tot}\left(1+\left[\frac{\pi^2}{3}-1\right]\Omega\right) \tag{3.64}$$

So we see that the rotation of the BEC tends to increase its radius, which could be expected, and therefore its total mass. Given a certain angular velocity ω, the maximum radius is once again fully defined by two parameters, the axion mass and the strength of the self-interaction. The equilibrium radius comes from the balance between two phenomena. On the one hand, the mass of the axions tends to collapse the cluster. On the other band, the repulsive self-interaction counters the collapse and allows the BEC to remain stable. In the rotating case, the self-interaction is helped by the rotation of the cluster. For high angular velocity, the model predicts a growth of the radius as $\sim \omega^{2/3}$. However one may expect that above a given threshold the condensation disappears. The scaling of the maximum radius and total mass of cluster for low ω are depicted in Figure 3.5.

3.2.3 Beyond the TF approximation

One may reasonably ask the question "What if we cannot neglect the kinetic term in the Gross-Pitaevskii equation ?". The resolution of a Schrödinger-like equation, in this case the Gross-Pitaevskii equation, assuming spherical symmetry follows a well-known procedure. First, we define the sought wavefunction

$$\Psi(\boldsymbol{r},t) = R(r)Y(\theta,\phi) \tag{3.65}$$

where $R(r)$ is the radial wave-function of the BEC and $Y(\theta,\phi)$ the angular dependence. As is usually the case, for the ground state the Y function is just a factor and we will absorb it in the normalisation factor to be found later. One shall notice that "Ψ" is the wave-function of the ground state. We did not re-use the notation 'Ψ_0" in order to avoid confusion with the solution found in the previous section, which will be used in this part of the work. Rewriting the comprehensive Gross-Pitaevskii equation (2.26) in spherical coordinates leads to:

$$-\frac{1}{2m_a r^2}\frac{d}{dr}r^2\frac{dR}{dr} + \left[V(r) + g|\Psi(r,t)|^2\right]R = \mu R \tag{3.66}$$

Introducing the function $X = rR$ allows to obtain the following equation which is similar to the Schrödinger equation in one dimension.

$$\frac{1}{2m_a}\frac{d^2\chi(r)}{dr^2} + \left[\mu - V(r) - g|\Psi|^2\right]\chi(r) = 0 \tag{3.67}$$

Let us take a closer look at the potential term. Due to its form, the equation is non-linear in $\chi(r)$. Adding the fact that the gravitational self-trapping implies that $V(r)$ is also a function of $\chi(r)$, we are one more time led to perform some approximations to solve this equation. To do so, one can use a series expansion of the potential and only keep

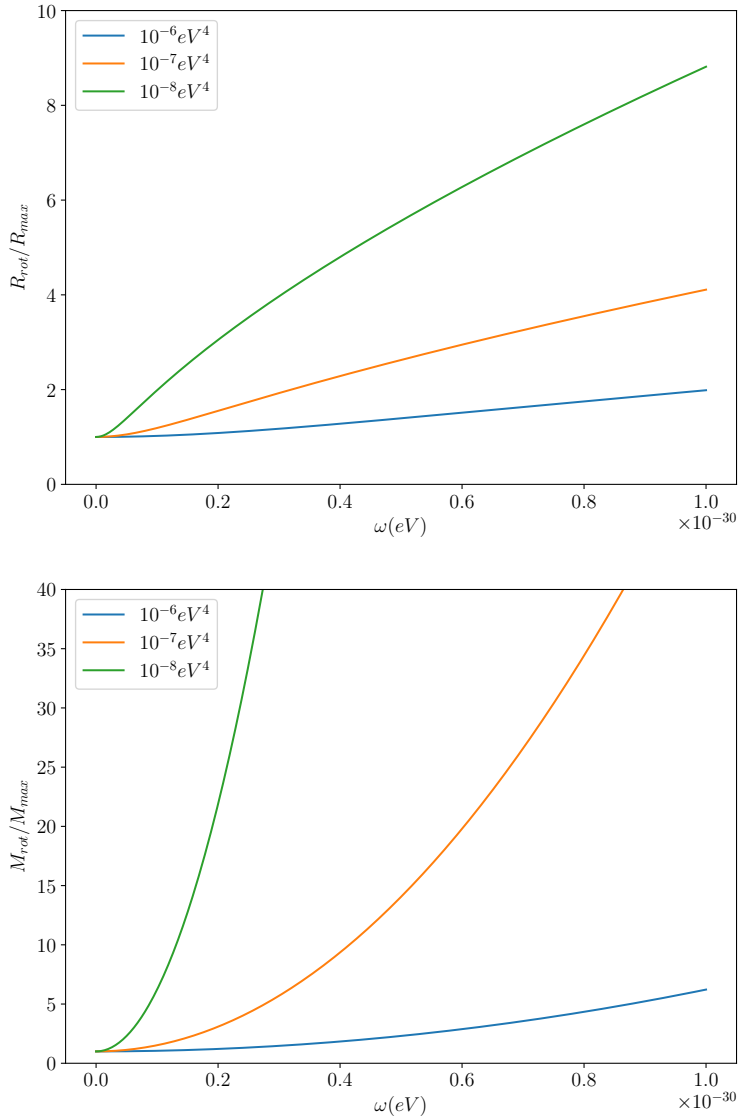

Figure 3.5: Maximum radius (top) and total mass (bottom) of a rotating BEC normalized by the radius and mass of a non-rotating one. They were plotted for three plausible densities of dark matter.

the first terms corresponding to the ones depending of Ψ_0, the wave-function obtained in the TF approximation. Therefore we can write (3.67)

$$\frac{1}{2m_a}\frac{d^2\chi(r)}{dr^2} + \left[\mu + 4\pi\frac{Gm_a^2}{r}\int_0^r |\Psi_0(r)|r^2\, dr - g|\Psi_0|^2\right]\chi(r) = 0 \tag{3.68}$$

We are now able to substitute $|\Psi_0|^2$ with its expression (3.53) to obtain the differential equation for $\chi(r)$

$$\frac{1}{2m_a}\frac{d^2\chi(r)}{dr^2} + \left[\mu + \frac{NGm_a^2}{\pi r}(\sin\kappa r - \kappa r\cos\kappa r) - g\frac{\kappa^2 N}{4\pi^2}\frac{\sin\kappa r}{r}\right]\chi(r) = 0 \tag{3.69}$$

Replacing κ by the definition given in section 3.2.1, one get the following equation to solve

$$\frac{d^2\chi(r)}{dr^2} + 2m_a\left[\mu - \frac{NGm_a^2\kappa}{\pi}\cos\kappa r\right]\chi(r) = 0 \tag{3.70}$$

This equation is in fact Hill's equation

$$\frac{d^2y(x)}{dx^2} + (\lambda + Q(x))\; y(x) = 0 \tag{3.71}$$

Hill's equations, notably used by H.G Hill to study the motion of the lunar perigee [65], encompass the class of homogeneous linear second-order differential equations with real periodic coefficients. As they possess numerous common features with the Sturm-Liouville theory, Hill's equations can for instance reduce to Mathieu's equations. We should not reasonably hope to find an analytical solution for the general equation (3.71). However, using the general theory developed around Hill's equation, one can discuss important properties of the solutions and hope to find approximate or numerical solutions. A rapid numerical verification shows that the correction is not very important (less than 1%) and we should neglect it to ease our work.

3.3 Trapping by Galaxies and Black Holes

We will not start to discuss at great length a model with a relativistic approach to gravity. However, for the sake of completeness, we should mention some interesting tracks. At the beginning of this chapter, we studied how a BEC of axions can be trapped under its own gravity. Although easier to describe, isolated clusters of dark matter have not been observed yet. However, dark matter also accounts for most of the mass inside galaxies. Thus, we should study the trapping of a BEC by the gravitational potential of a galaxy. One will encounter two issues in trying to do so.

Firstly, the shapes encountered among galaxies are not unique. Therefore their inner structures and dynamics cannot be described by a unique analytical potential. Secondly, even for a common shape of galaxy such as a spiral one, the structure can exhibit a high degree of sophistication. As a matter of fact, one shall consider the arms, the bulge, the disk and the loss of the spherical symmetry among others details. Further more, spiral galaxies harbour super-massive black holes. Facing such difficulties, one should begin by adding simple features to our model. The simplest one would be to add a spherically

symmetrical potential well to the one created by the cloud of axions. This potential would account for the baryonic contribution to the trap as well as the central black hole. On galactic scales, it is equivalent to adding a Newtonian potential term to our equations. We may expect an enhancement of the trapping and thus, for a given mass, smaller and denser clusters of particles. Nevertheless, we should carefully treat the area near the centre of the potential where we cannot simply add a Newtonian term for a certain class of objects: black holes. Moreover, the baryonic contribution itself depends on the density profile of the BEC. We thus have to take into account the retro-action of one type of matter on the other and vice-versa. It is quite easy to modify Equations (3.46) to add a baryonic contribution to Poisson's equation.

$$\Delta\Phi = 4\pi G(\rho_{DM} + \rho_{Bar}) \tag{3.72}$$

Applying the Laplacian operator the Gross-Pitaevski equation as in our first model, one gets

$$4\pi G(\rho_{DM} + \rho_{Bar})m_a + \frac{g}{m_a}\Delta\rho_{DM} = 0 \tag{3.73}$$

This system of two differential equations may then be solved to provide a better approximation than the one in Section 3.2.1. We also mentioned the issues that could arise near the central black hole, when Newtonian gravity shatters. To correctly treat this area, one should first modify the action of our field into a covariant one

$$S = \int \mathcal{L}\sqrt{-g}\; d^4x \tag{3.74}$$

where g is the determinant of the metric. It is simple to show that this expression is indeed covariant. By obtaining the Klein-Gordon equation in the General Relativity framework, one may obtain a Gross-Pitaevski type equation [66, 67]. This equation, implying the metric tensor, can then be numerically solved. One more time, this is out the scope of this thesis and is mentioned here to suggest different paths of investigation. However, we should first test our simplest model to check the consistency and credibility of our hypotheses.

4

Observational consequences

4.1 The SPARC Data

The observation of rotation curves can be difficult and cumbersome. The challenge consists in finding an appropriate tracer to map the gravitational potential around a galaxy, which is not a trivial task. Indeed, one has at one's disposal multiple tracers such as the CO transition lines, which lie in the millimetre wave range, or the SII and NII emission lines [68]. However, one of the best tracers is atomic hydrogen (HI) due to two mains advantages. HI is relatively cold and thus follows near by circular orbits with small velocity dispersion. Moreover, the HI contribution extends further from the galactic centre than stars or others gases [14]. The SPARC catalogue aims at gathering data from published papers and previous studies concerning rotation curves observed via atomic hydrogen. It consists in 175 late-type galaxies, most of which observed by the Spitzer Space Telescope.

Some data are not of interest for this Master thesis. We will restrict us to the description and commentary of the interesting ones. One of those important pieces of information is the Hubble type of the galaxies (see figure 1.3). Indeed, since our model is rather simple and does not include features such as a central bar, we should apply our equations to the most symmetric galaxies. As a consequence, we will restrict ourselves to a selection of 34 galaxies. Next, the data contain the rotation velocity for different radii as well as the contribution to this velocity from the bulge, the disk and the gas. However, those three contributions are normalised assuming a matter to light ration $\Upsilon_\star$ of 1. This is not the case for the bulge and the galactic disk and one should find appropriate ratios Υ_{bul} and Υ_{disk} consistent with multiple observations to compute the total baryonic contribution.

4.1.1 Data processing

The first step is to retrieve the interesting data from the SPARC catalogue, which can be found online [69]. To do so, a Python script was written to isolate the names of the most symmetric galaxies and their types. Here, a compromise had to be made between a low number of highly symmetrical galaxies and a large number of galaxies with all sizes and shapes. Taking those considerations into account, we limited our choice to four Hubble type, S0, Sa, Sb ,and Sc, which correspond to spiral and lenticular galaxies. Then, a second script was written to collect the velocities and baryonic contributions. Once those data were obtained, their were converted in the adequate units and the rotation curves were plotted.

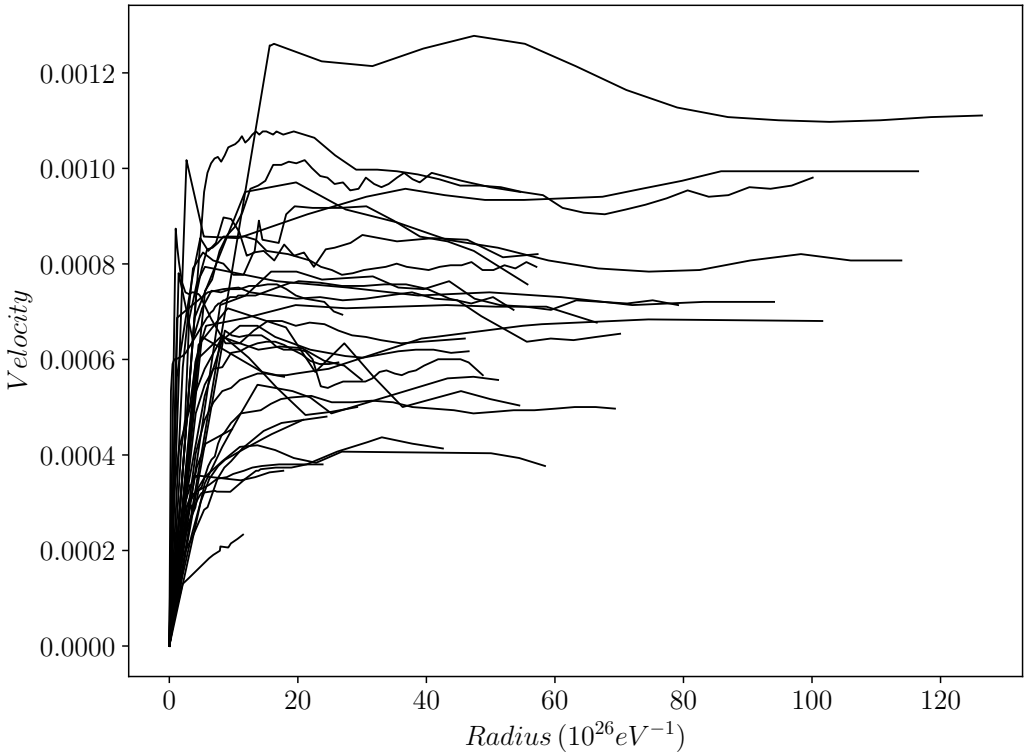

Figure 4.1: Rotation curves rebuilt using the SPARC data for our sample of galaxies.

4.2 Rotation curves

4.2.1 Baryonic contribution

One should compare our model to the rotation curves of galaxies. To compare our equations with actual data, we should derive the speed of a test particle as a function of the radius. In the Newtonian approximation, the velocity due to a spherical distribution of dark matter can be expressed as

$$V_{DM}(r) = \sqrt{\frac{GM_{DM}(r)}{r}} \tag{4.1}$$

The total rotation velocity can be decomposed into two contributions: the baryonic part due to M_B composed of gas, stars and dust and the dark matter part due to M_{DM}, that we assumed made of an axion BEC in this work. The baryonic contribution can be extracted from the SPARC data and is composed of the gas contribution, the bulge contribution and the disk contribution. The baryonic contribution to the rotation velocity is thus given by [14]

$$V_{bar} = \sqrt{V_{gas}|V_{gas}| + \Upsilon_{bul}V_{bul}|V_{bul}| + \Upsilon_{disk}V_{disk}|V_{disk}|} \tag{4.2}$$

The absolute values are necessary here because of negative contributions in the centre of some galaxies due to gas depression resulting in a stronger gravitational pull from outer regions. We decided here to take the experimental baryonic contribution but one should notice that it is also possible to use theoretical models for the baryonic matter profile of galaxies such as the one proposed in [70].

To compute this baryonic contribution, one should choose a value for the parameters Υ_{bul} and Υ_{disk}. Those two parameters are difficult to measure and explain theoretically. However, one may try to minimise the Baryonic Tully-Fisher relation with respect to Υ_{disk}, giving a value of 0.5 [71, 72]. We can then assume [14]

$$\Upsilon_{bul} = 1.4\Upsilon_{disk} \tag{4.3}$$

One should note that the correct evaluation of those two parameters is extremely difficult and no universal consensus exist nowadays. Moreover, those values are taken equal for all our galaxies but it could be otherwise.

4.2.2 Dark Matter contribution

The Dark Matter contribution to the rotation velocity can be expressed thanks to our model. Given the matter density (3.51), one can write the total mass of Dark Matter encompassed in a sphere of radius r as

$$M_{DM} = 4\pi \int_0^r \rho(r') r'^2 \, dr' \tag{4.4}$$

which leads after integration of the density profile to the following expression

$$M_{DM} = 4\pi\rho_0 \frac{\sin \kappa r - \kappa r \cos \kappa r}{\kappa^3} \tag{4.5}$$

Since κ is a function of m_a and λ, we still have three free parameters if we add to those two the central density of the axion cloud. We thus have a contribution to the velocity by the Dark Matter given by

$$V_{DM} = \sqrt{4\pi G\rho_0 \frac{\sin \kappa r - \kappa r \cos kr}{r\kappa^3}} \tag{4.6}$$

with our usual κ defined earlier as $\sqrt{\frac{Gm_a^3}{a_s}}$.

4.2.3 Model calibration

A simple but easy to implement calibration method is a non-linear least-squares fit. Our null hypothesis will be in this case: the theoretical distribution of velocity predicted by our model is the real one, i.e. the theoretical distribution of velocity fits the observed data well. Obviously one should note that the test allows us to reject our null hypothesis H_0 but not confirm it. The idea is to compute the following statistics

$$\chi^2 = \sum_i^n \left(\frac{V_i^{th} - V_i^{obs}}{\sigma} \right)^2 \tag{4.7}$$

In fact, we will preferably use the reduced χ^2 statistics, which takes into account the number of points n for a galaxy as well as the number of degrees of freedom p.

$$\chi^2_{red} = \frac{\chi^2}{n - p} \tag{4.8}$$

We optimised this function of the three parameters m_a, λ, and ρ_0. One can then compare the value of our χ^2_{red} with a chosen threshold. For instance, if one gets a value $X^2_{red} = 7.81$ for three degree of freedom, one may reject the null-hypothesis with a certitude of 95%.

Although this statistical test was used in many papers on the topic, we should emphasise that it may not be the best way to calibrate the model, as is suggested in [73]. However, the main idea of this work is to develop the theoretical ground while looking at the coherence of the model and not giving a final answer concerning BEC of axions. We thus restrict ourselves to this simple statistical analysis. The ones wishing to go further into the analysis are invited to follow the track of [74]. Bayesian statistics and more complex algorithms can indeed be of great use for this kind of computation [75].

4.2.4 Results

In this section, the main results will be presented. Their discussion is kept for the next section. Multiple graphs showing the theoretical and observed contributions from dark matter to the rotation velocity may be found in appendix. One of those curves is shown in Figure 4.2. A badly fitted curves is also shown. Table 4.1 shows the best-fitting parameters for our sample of galaxies as well as the χ^2 value. As mentioned in the previous section, the three free parameters were the mass of the particle, the interaction parameter and the central density of the DM halos. The $\log_{10} m_a$ lies around -23.3 with a standard deviation of 1.4. The mean value for $\log_{10} \lambda$ is -70.9 with a standard deviation of 4.01 among the galaxy sample. Finally, the fitted central density $\log_{10} \rho_0$ was on average -7.5 with a standard deviation of 0.9

4.2.5 Discussion

We shall now discuss our results more extensively. We made the hypothesis that dark matter in galaxies was a Bose-Einstein condensate of ultralight particles with extremely weak self-interaction. Such particles are expected to have a very weak mass lying around 10^{-22} eV [60]. As one can see on Table 4.1, the estimated parameters are in the expected range for an ultralight axion or another ALPs with an average mass of $\sim 10^{-23}$ eV. We should emphasise that this result agrees with other studies of the BEC model such as [74].

Concerning the interaction parameter, we developed this model expecting an extremely weak repulsive interaction and thus a weak value of λ. The mean estimated interaction parameter lies around 10^{-70}, which is indeed almost negligible compared to the value of the mass. If we look at the mean value found for the central density of the dark matter halo, we obtain a value of approximately $10^{-7.5}$ eV^4. This value is also plausible. For instance, the local density of dark matter in the solar system is more or less 10^{-6} eV^4 [76]. It is an order of magnitude larger than the fitted density obtained. However, most of the galaxies in our sample are smaller than the Milky Way. While we should be cautions about the obtained value, it is not an unrealistic result either. A plot of the different galaxies in the (m_a, λ) and (m_a, ρ_0) plans is shown in Figure 4.4. One can observe a clustering of the fitted values.

If the mean values obtained for our parameters are satisfying, we should concern ourselves with the statistical quality of the fit and with the likelihood for such parameters to be the right ones. To perform the analysis, we will look at the χ^2 statistics. The χ^2 value is under 2 for ten galaxies. Seven galaxies lie between 2 and 10 while the others are far from what could be called a good fit. We will start by discussing the group of ten well-fitted galaxies. One could ask if the Hubble type of the galaxy impacts the performance

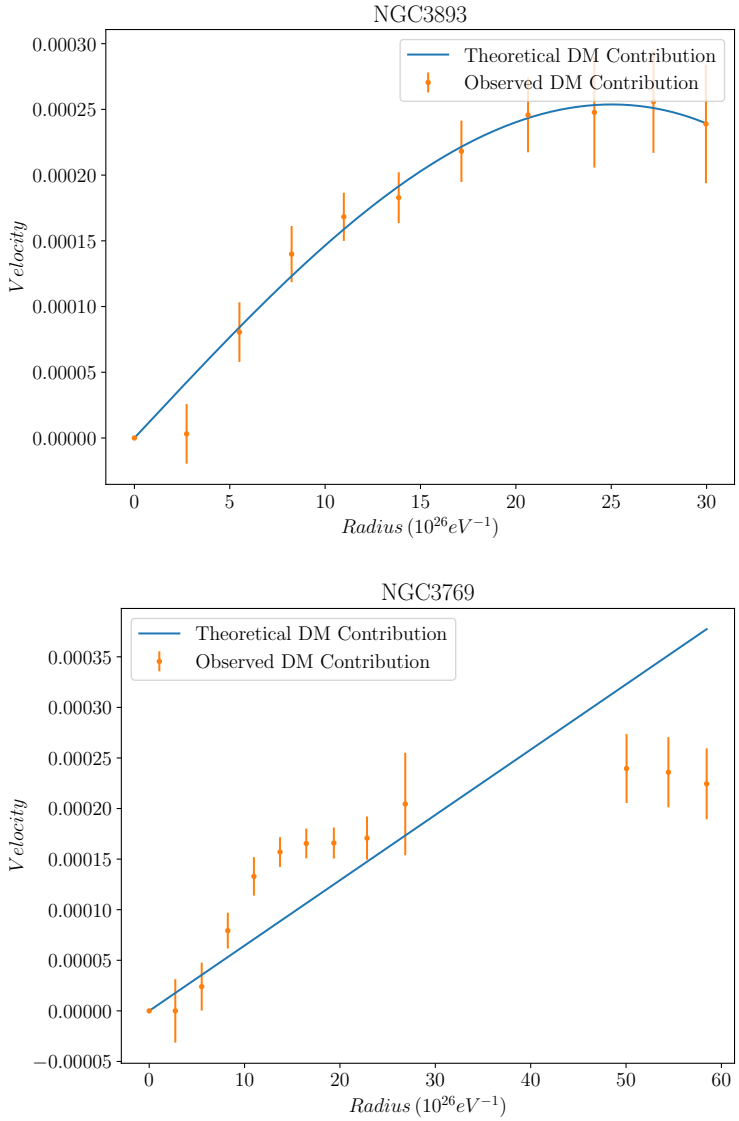

Figure 4.2: Top: observed and theoretical DM contribution to the rotation velocity for the galaxy NGC 3893. Bottom: A badly fitted curve. In this case the model is unable to fit the data. Other fitted rotation curves may be found in appendix

Id	$\log_{10} m_a/1$ eV	$\log_{10} \lambda$	$\log_{10} \rho_0/1$ eV^4	χ^2_{red}
F568-1	-23.09 ± 0.02	-76.41 $\pm$ 0.07	-6.40 ± 0.11	0.6
F571-8	-21.77 ± 2.04	-62.05 ± 5.36	-7.19 ± 0.06	19.6
F579-V1	-21.44 ± 0.01	-71.16 ± 0.02	-5.28 ± 0.14	0.6
F583-4	-21.21 ± 0.04	-68.96 ± 0.24	-7.17 ± 0.12	0.8
NGC0024	-21.76 ± 2.14	-62.07 ± 6.21	-7.21 ± 0.09	14.4
NGC0801	-23.75 ± 1.61	-70.53 ± 7.44	-8.54 ± 0.05	13.8
NGC0891	-24.35 ± 1.93	-72.33 ± 6.15	-7.87 ± 0.06	21.2
NGC2683	-24.23 ± 1.91	-72.26 ± 7.26	-7.92 ± 0.10	11.9
NGC2841	-24.38 ± 1.80	-72.46 ± 6.59	-7.83 ± 0.03	70.6
NGC2955	-23.92 ± 1.66	-71.99 ± 8.13	-8.19 ± 0.20	4.9
NGC2976	-21.71 ± 1.66	-65.46 ± 8.77	-6.81 ± 0.18	0.4
NGC2998	-24.48 ± 1.94	-72.44 ± 6.18	-8.09 ± 0.03	24.8
NGC3198	-23.14 ± 0.01	-75.85 ± 0.01	-7.25 ± 0.03	39.5
NGC3726	-23.98 ± 1.66	-71.93 ± 8.09	-8.13 ± 0.11	2.0
NGC3769	-24.28 ± 1.91	-72.48 ± 7.46	-8.01 ± 0.11	9.7
NGC3877	-24.38 ± 2.25	-72.46 ± 6.43	-7.83 ± 0.15	10.8
NGC3893	-21.73 ± 0.04	-70.30 ± 0.20	-7.25 ± 0.10	0.5
NGC4013	-24.19 ± 1.75	-72.21 ± 7.42	-7.94 ± 0.06	1.1
NGC4085	-26.56 ± 1.87	-82.87 ± 7.82	-7.71 ± 0.20	5.8
NGC4138	-21.19 ± 0.01	-72.32 ± 0.01	-3.20 ± 0.14	0.7
NGC4157	-24.32 ± 1.83	-72.63 ± 7.46	-8.05 ± 0.12	0.5
NGC4217	-25.65 ± 0.03	-69.62 ± 0.11	-8.37 ± 0.19	31.6
NGC5033	-24.27 ± 1.86	-72.28 ± 6.63	-7.90 ± 0.02	89.9
NGC5907	-24.19 ± 1.72	-72.13 ± 6.77	-8.13 ± 0.02	75.7
NGC5985	-21.83 ± 1.51	-64.05 ± 7.69	-7.40 ± 0.03	103.5
NGC6195	-23.26 ± 1.32	-70.10 ± 9.21	-8.45 ± 0.14	2.3
NGC6674	-21.42 ± 0.01	-67.96 ± 0.03	-7.84 ± 0.01	44.9
NGC7331	-24.25 ± 1.75	-72.01 ± 6.86	-8.10 ± 0.05	7.9
UGC02487	-24.32 ± 1.63	-72.53 ± 6.63	-7.95 ± 0.01	167.6
UGC02885	-21.80 ± 0.02	-69.38 ± 0.10	-7.86 ± 0.07	4.2
UGC03546	-24.62 ± 2.12	-72.69 ± 5.46	-7.72 ± 0.02	9.2
UGC03580	-24.36 ± 1.96	-72.36 ± 5.58	-7.86 ± 0.04	37.1
UGC06614	-22.50 ± 0.09	-72.03 ± 13.56	-8.16 ± 0.14	1.1
UGC06786	-21.85 ± 1.52	-64.05 ± 7.65	-7.38 ± 0.02	59.0

Table 4.1: Estimated parameters for our galaxy sample as well as their confidence interval.

of the model. Looking at our group of ten galaxies, it appears that it does not depend strongly of the type (and thus of the symmetry) of the galaxy. How could we explain this? One should remember that Dark Matter only interact weakly with baryonic matter. The interaction between the two kinds of matter is mainly gravitational. Thus, the small asymmetries such as arms in the baryonic matter distribution could be neglected.

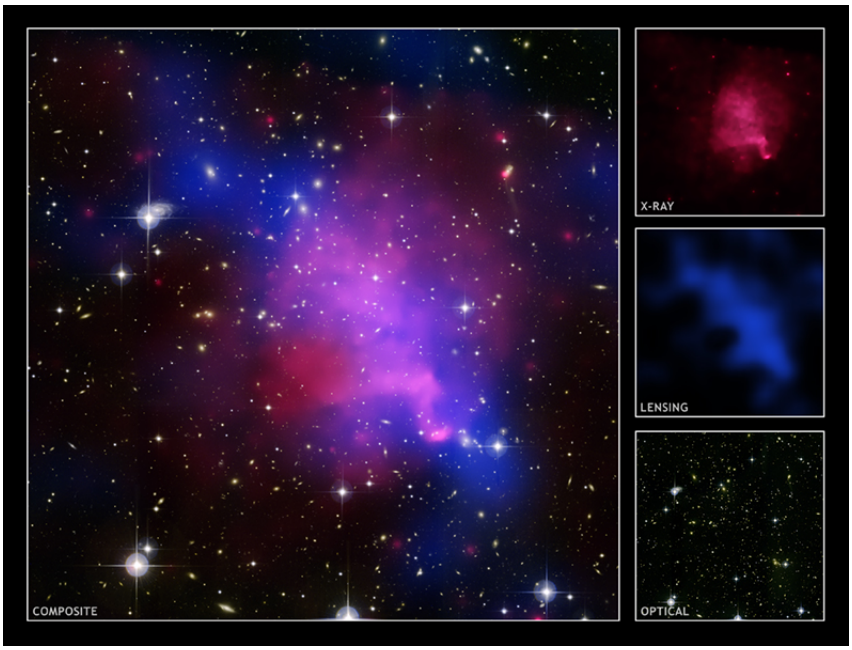

Figure 4.3: Abel 520, which consists in two cluster of matter colliding. Such collisions could lead to the destruction of the Bose-Einstein condensate [77].

However, if the χ^2 is convincing, the confidence intervals on the parameters do not allow to draw a strong conclusion. Indeed, the error margins found for the different galaxies do not overlap and thus it may be daring to make strong statements on those results. Moreover, if one looks at the rotation curves in Appendix A, one can observe that the discrepancies between the model and the observed dark matter contribution are more glaring at short radius. How could we explain those different observations? The reader should remember that our model is an overly simplified one. We neglected asymmetries, the modification of the trapping by baryonic matter, the central black holes contained at the heart of galaxies as well as general relativistic considerations. It could be useful to develop the model more precisely to verify if such details may correct the short-radius issues of the model. One may also note from the rotation curves in Appendix A that some curves such as the one from NGC4013 exhibit oscillations. The model obviously does not explain those. Perhaps these are due to the caustic rings,i.e. over-densities in the dark matter density profile caused by the in-fall of dark matter into galaxies [78].

Apart from those ten galaxies, the last 24 cannot be fitted correctly by the model. We should here reflect on what could explain such a difference between galaxies. At least two interesting pathways may be explored here. On the one hand, we could make the hypothesis that dark matter is not a unique kind of particles but a family of different particles. Such multi-component dark matter could easily emerge from extensions of the Standard Model [43]. Indeed, as explained in Chapter 1, symmetry breaking may give rise to a broad range of particles. On the other hand, it is possible that events such

as collisions between galaxies, as shown in Figure 4.3, or a high number of supernovae have ejected dark matter and destroyed the condensate. Each galaxies having its own history and specificity, it is difficult to draw conclusion concerning those galaxies and the efficiency of the model. We discuss ideas for future works in the next chapter.

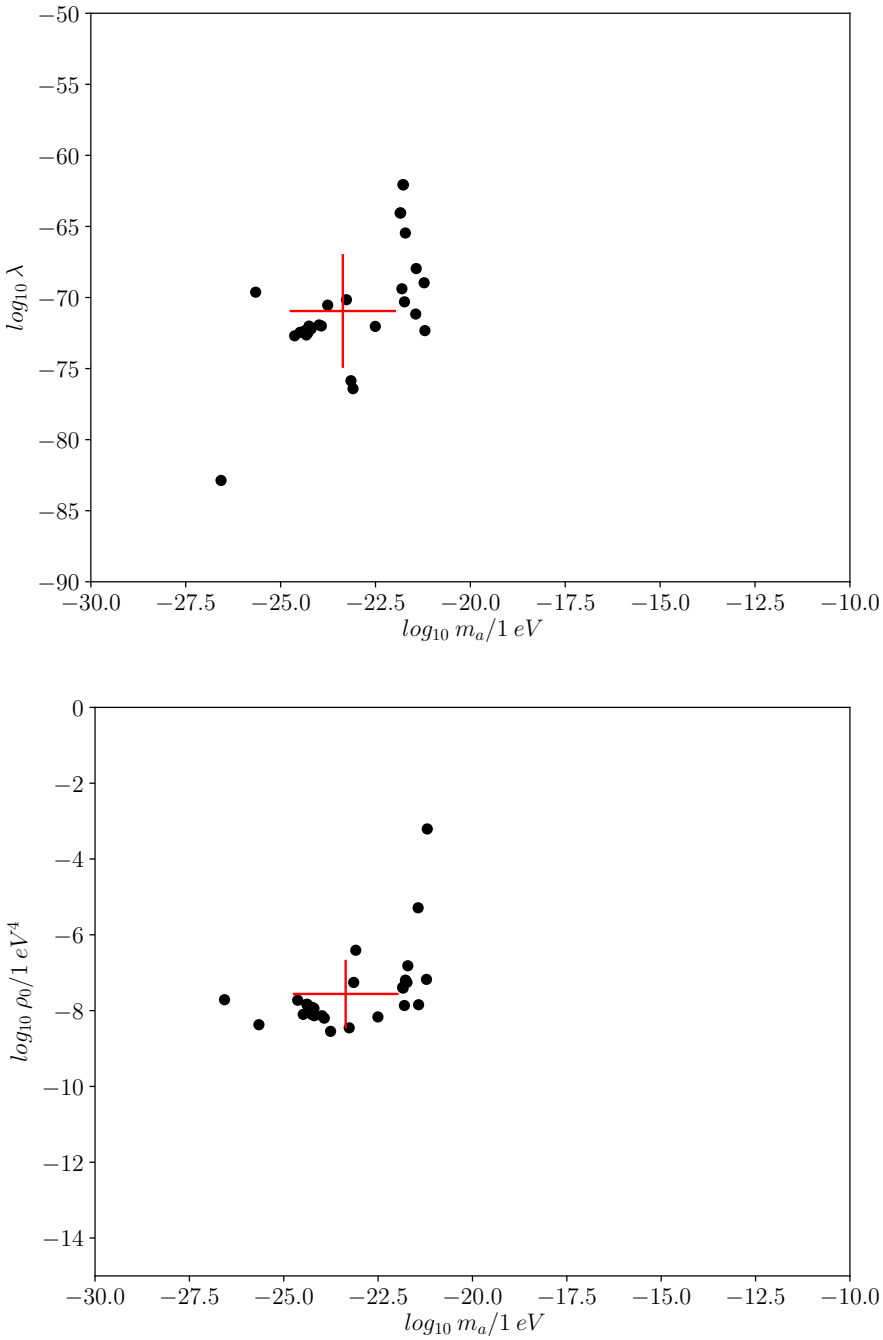

Figure 4.4: Top: scattering plot of the obtained parameters with the masses in abscissa and interaction parameters in ordinate. The centre of the cross is the mean mass and λ value. The arms of the cross show one standard deviation. Bottom: same plot for the masses and the central densities.

5

Conclusion

It is now time to summarise our journey through the Bose-Einstein condensation of axions and draw some conclusions on our work. We aimed at synthesising and comparing to the observation a specific model of dark matter, a BEC of axions. This master thesis started by recalling some evidence in favour of dark matter. The possible origin of the axion was discussed as well as why it is an interesting candidate. We have seen that the existence of ultralight scalar bosons was predicted by multiple extensions of the Standard Model thanks to symmetry breaking.

We then introduced the BEC theories and some interesting equations and properties of such systems. It allowed us to discuss the case of axions in Chapter 3. We have seen that the condensation of axions was indeed possible if we imposed some condition on the self-interaction. We showed that despite the repulsive self-interaction needed to form a stable condensate, the Universe could exhibit a sufficient lifetime. We also concluded that the usual QCD axion could not form a galactic-size condensate. Subsequently we derived a solution for the wavefunction and the density profile of the BEC inside a gravitational trap. We have seen that such a solution predict a unique radius for the dark matter halo has a function of m_a and λ. We ended this chapter by solving the Gross-Pitaevski equation for a slowly rotating BEC and taking a look beyond the Thomas-Fermi approximation.

The next chapter was dedicated to the comparison of our model to actual data. We used the SPARC database to obtain the observed Dark Matter contribution to the rotation of galaxies and then tried to fit those data with our simplified model. We noticed a clustering in the parameter space around a mean mass of $10^{-23.3}$ eV and an mean interaction parameter of $10^{-70.9}$. Those results were consistent with our initial hypotheses. However, two thirds of the galaxies had a χ^2_{red} too high to draw sensible conclusions on our model's validity. Further investigations are thus needed.

Concerning the description of the BEC, we neglected a lot of different features such as fast rotation of galaxies or more complex gravitational traps. One could numerically study more realistic galactic trapping and thus improve our results. We also did not take into account some known phenomena such as caustic rings. We quickly mentioned phonons through the condensate and laid the ground for further studies. These phonons could give rise to intriguing coupling between baryonic sources and long-range interaction.

One could add layers of complexity by studying events such as galactic collisions and thus collisions between two condensates, or multi-component dark matter. Indeed, a

mixing of laser-trapped BEC often exhibit unusual behaviour such as coupling between different components [79] or even multiple macroscopic eigenvalues for the density matrix [80]. We treated gravitation in the Newtonian regime to describe the trap. Moreover, we did not describe the central black holes at the heart of certain galaxies. Working with a curved background could lead to improvement of the model and the emergence of new phenomena [66]. On the observational side, the polarisation of light by dark matter has been studied in the case of a cloud of axions. One could study the hypothetical effect if this cloud is condensed.

As one can see, there is an endless list of further studies possible. We only talked about new Physics but we could also perform a deeper and more rigorous statistical analysis of the results for our simple model. We only looked at some basic features of our results. However, it could be appropriate to inspect the error bar on the different parameters and carry out a more comprehensive discussion about the credibility of the model. The topic of BEC of axions is thus promising and abounds with beautiful Physics. Moreover, it brings insight into what dark matter could be while unravelling curious consequences and phenomena. If the riddle is far from being solved, we continue to probe deeper and deeper into the mystery of dark matter. New experiments flourish each year and the quest for the solution will surely lead to a great breakthrough one day or the other.

A

Rotation curves and DM contributions

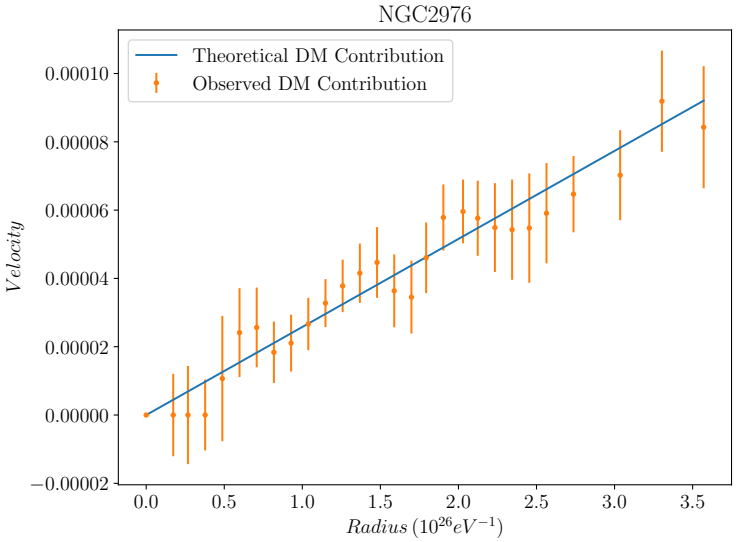

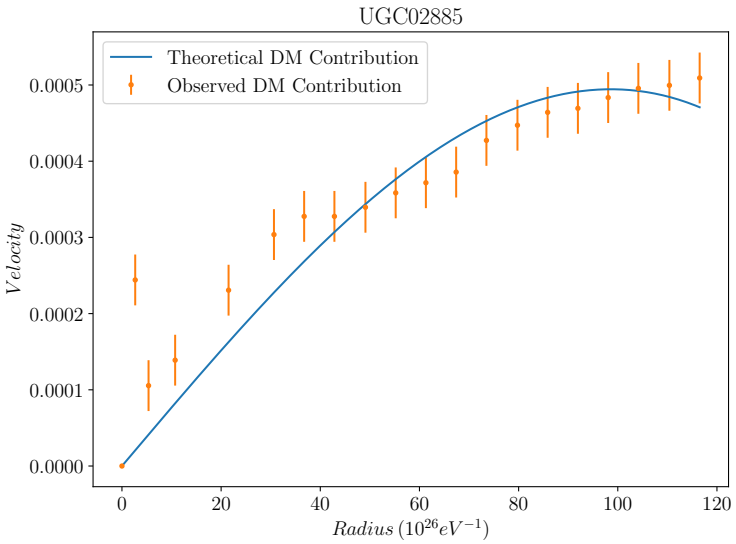

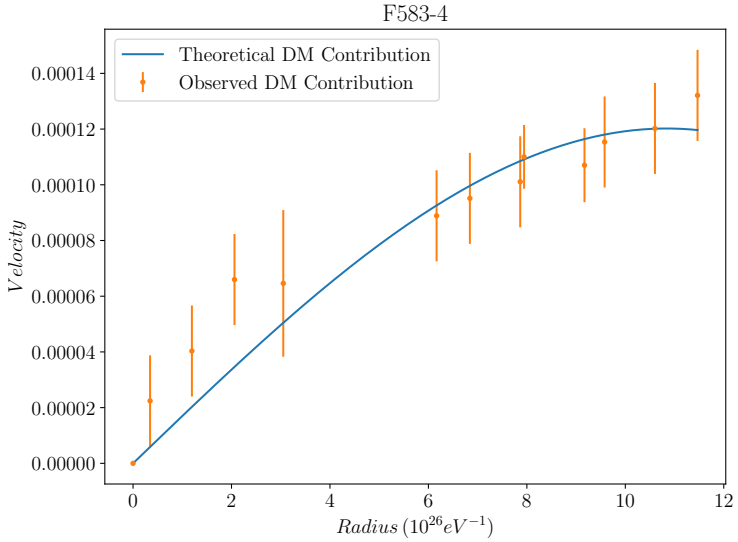
F583-4
Theoretical DM Contribution
Observed DM Contribution
Velocity
0.00014
0.00012
0.00010
0.00008
0.00006
0.00004
0.00002
0.00000
0
2
4
6
8
10
12
Radius ($10^{26} eV^{-1}$)

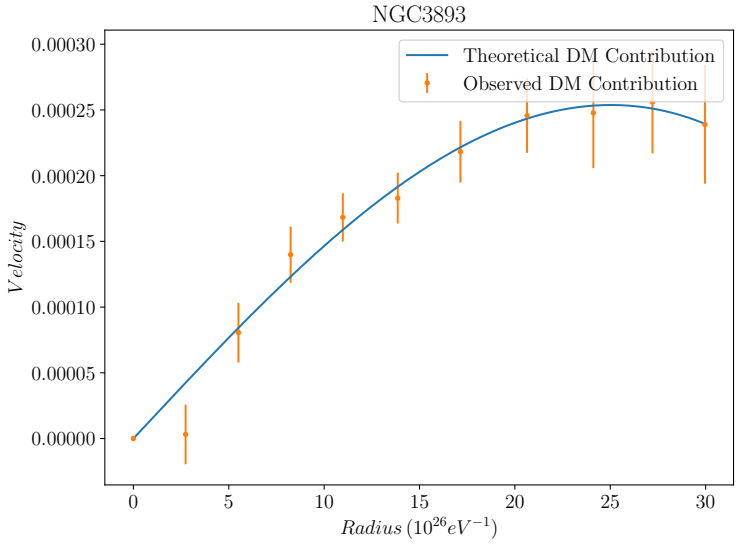
NGC3893
Theoretical DM Contribution
Observed DM Contribution
Velocity
0.00030
0.00025
0.00020
0.00015
0.00010
0.00005
0.00000
0
5
10
15
20
25
30
Radius ($10^{26} eV^{-1}$)

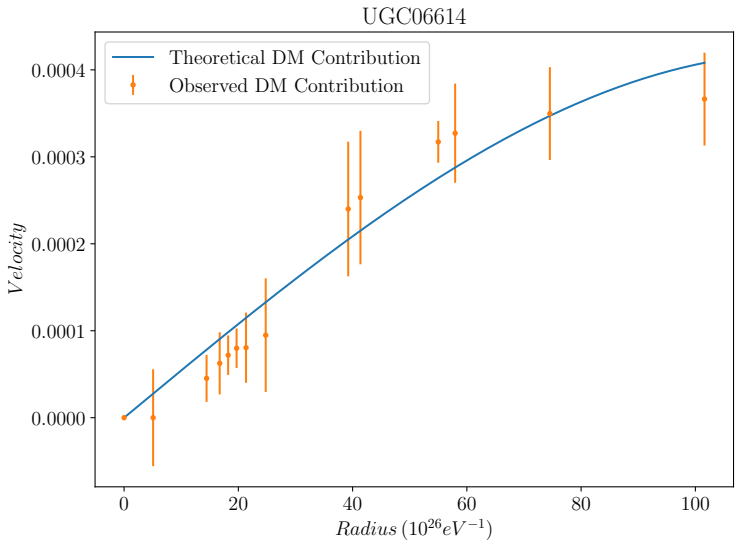
UGC06614
Theoretical DM Contribution
Observed DM Contribution
Velocity
0.0004
0.0003
0.0002
0.0001
0.0000
0
20
40
60
80
100
Radius ($10^{26} eV^{-1}$)

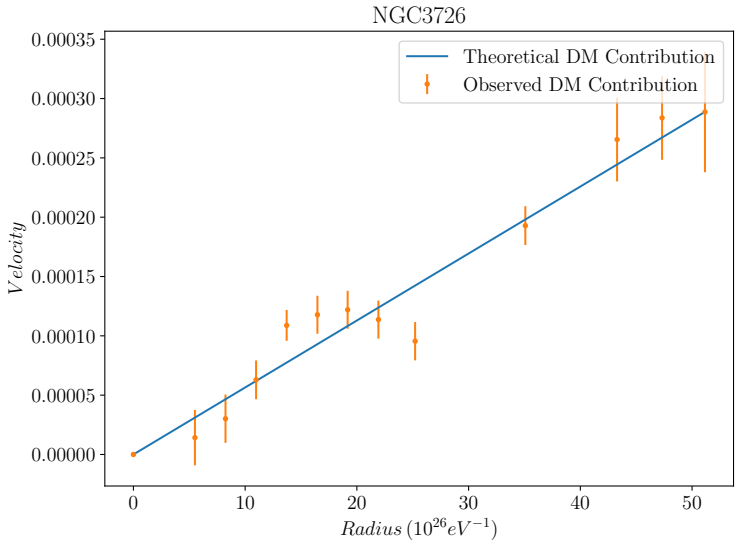
NGC3726
Theoretical DM Contribution
Observed DM Contribution
Velocity
Radius ($10^{26} eV^{-1}$)
0.00035
0.00030
0.00025
0.00020
0.00015
0.00010
0.00005
0.00000
0
10
20
30
40
50

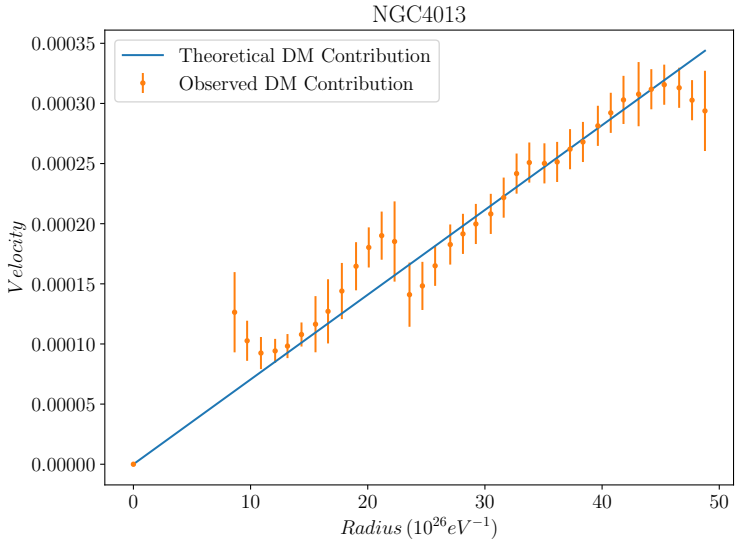
NGC4013
Theoretical DM Contribution
Observed DM Contribution
Velocity
Radius ($10^{26} eV^{-1}$)
0.00035
0.00030
0.00025
0.00020
0.00015
0.00010
0.00005
0.00000
0
10
20
30
40
50

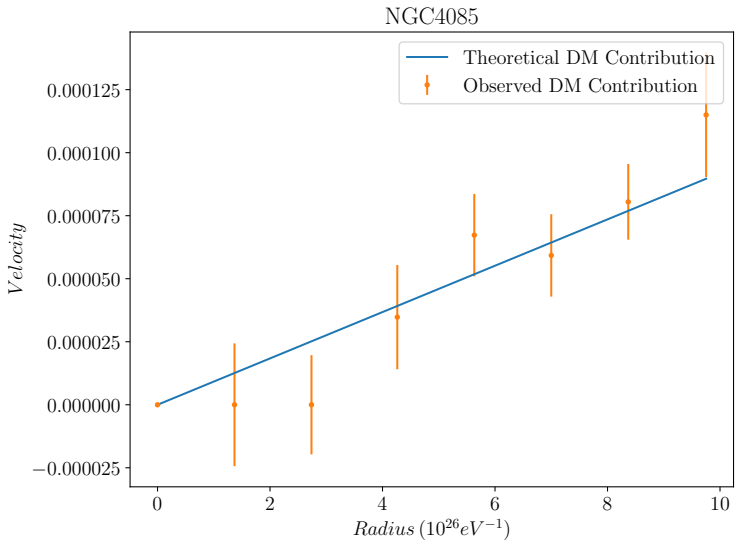
NGC4085
Theoretical DM Contribution
Observed DM Contribution
Velocity
Radius ($10^{26} eV^{-1}$)
0.000125
0.000100
0.000075
0.000050
0.000025
0.000000
−0.000025
0
2
4
6
8
10

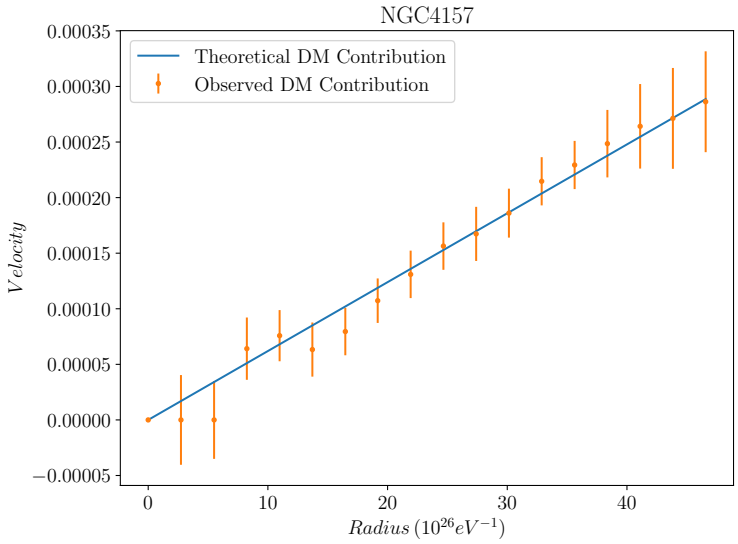
NGC4157
Theoretical DM Contribution
Observed DM Contribution
Velocity
Radius ($10^{26} eV^{-1}$)
0.00035
0.00030
0.00025
0.00020
0.00015
0.00010
0.00005
0.00000
−0.00005
0
10
20
30
40

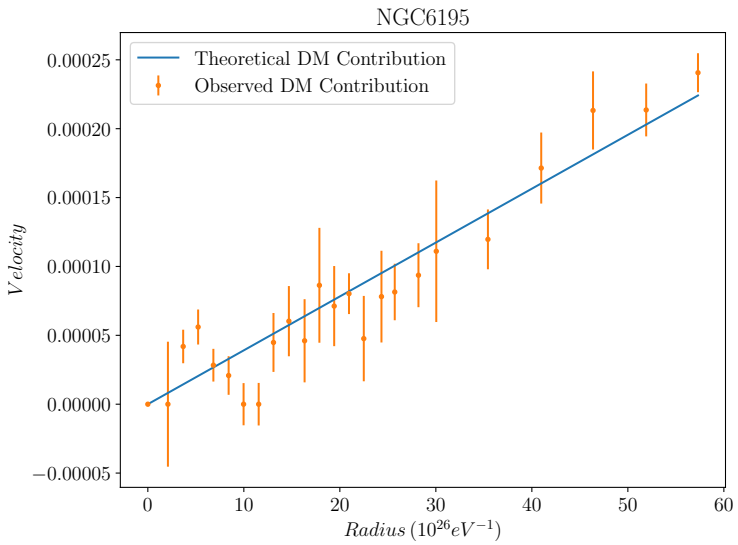
NGC6195
Theoretical DM Contribution
Observed DM Contribution
Velocity
Radius ($10^{26} eV^{-1}$)
0.00025
0.00020
0.00015
0.00010
0.00005
0.00000
−0.00005
0
10
20
30
40
50
60

Bibliography

[1] D. Dominguez. (2015). "Particles of the standard model of particle physics," [Online]. Available: `https://home.cern/science/physics/standard-model` (visited on 07/05/2021).

[2] F. Wilczek, "Problem of Strong P and T Invariance in the presence of instantons," *Phys. Rev. Lett.*, vol. 40, pp. 279–282, 5 Jan. 1978.

[3] P. Woit. (2015). "The West Coast Metric is the wrong one," [Online]. Available: `https://www.math.columbia.edu/~woit/wordpress/?p=7773` (visited on 04/09/2021).

[4] G. Bertone and D. Hooper, "History of dark matter," *Rev. Mod. Phys.*, vol. 90, p. 045 002, 4 2018.

[5] S. van den Bergh, "The early history of dark matter," *Publications of the Astronomical Society of the Pacific*, vol. 111, no. 760, pp. 657–660, 1999.

[6] J. G. de Swart, G. Bertone, and J. van Dongen, "How dark matter came to matter," *Nature Astronomy*, vol. 1, no. 3, p. 0059, 2017.

[7] W. Thomson, *Baltimore Lectures on molecular dynamics and the wave theory of light*. Cambridge University Press, 1884, pp. 267–278.

[8] J. H. Oort, "The force exerted by the stellar system in the direction perpendicular to the galactic plane and some related problems," *Bull. Astron. Inst. Netherlands*, vol. 6, pp. 249–287, 1932.

[9] F. Zwicky, "Die Rotverschiebung von extragalaktischen Nebeln," *Helvetica Physica Acta*, vol. 6, pp. 110–127, Jan. 1933.

[10] V. C. Rubin, J. Ford W. K., and N. Thonnard, "Extended rotation curves of high-luminosity spiral galaxies. IV. Systematic dynamical properties, Sa-Sc.," *APJL*, vol. 225, pp. 107–111, Nov. 1978.

[11] P. Young, J. E. Gunn, J. Kristian, J. B. Oke, and J. A. Westphal, "The double quasar Q0957+561 A, B: a gravitational lens image formed by a galaxy at z=0.39.," *The Astrophysical Journal*, vol. 241, pp. 507–520, Oct. 1980.

[12] H. Hoekstra, M. Bartelmann, H. Dahle, H. Israel, M. Limousin, and M. Meneghetti, "Masses of galaxy clusters from gravitational lensing," *Space Science Reviews*, vol. 177, no. 1, pp. 75–118, 2013.

[13] S. Ettori, A. Donnarumma, E. Pointecouteau, T. H. Reiprich, S. Giodini, L. Lovisari, and R. W. Schmidt, "Mass profiles of galaxy clusters from x-ray analysis," *Space Science Reviews*, vol. 177, no. 1, pp. 119–154, 2013.

[14] F. Lelli, S. S. McGaugh, and J. M. Schombert, "SPARC: Mass Models for 175 Disk Galaxies with Spitzer Photometry and Accurate Rotation Curves," *The Astrophysical Journal*, vol. 152, no. 6, p. 157, Dec. 2016.

[15] R. B. Tully and J. R. Fisher, "Reprint of 1977A&A....54..661T. A new method of determining distance to galaxies.," *Astronomy and Astrophysics*, vol. 500, pp. 105–117, Feb. 1977.

[16] S. S. McGaugh, "The baryonic Tully-Fisher relation of galaxies with extended rotation curves and the stellar mass of rotating galaxies," *The Astrophysical Journal*, vol. 632, no. 2, pp. 859–871, Oct. 2005.

[17] S. Torres-Flores, B. Epinat, P. Amram, H. Plana, and C. Mendes de Oliveira, "GHASP: an H-alpha kinematic survey of spiral and irregular galaxies – IX. The near-infrared, stellar and baryonic Tully–Fisher relations*," *Monthly Notices of the Royal Astronomical Society*, vol. 416, no. 3, pp. 1936–1948, Sep. 2011, ISSN: 0035-8711.

[18] E. Hubble, "No. 324. Extra-galactic nebulae.," *Contributions from the Mount Wilson Observatory / Carnegie Institution of Washington*, vol. 324, pp. 1–49, Jan. 1926.

[19] NASA and ESA. (2016). "Anatomy of the milky way," [Online]. Available: `https://sci.esa.int/web/gaia/-/58206-anatomy-of-the-milky-way` (visited on 05/05/2021).

[20] N. Aghanim, Y. Akrami, M. Ashdown, J. Aumont, C. Baccigalupi, M. Ballardini, A. J. Banday, R. B. Barreiro, N. Bartolo, and et al., "Planck 2018 results," *Astronomy Astrophysics*, vol. 641, A6, Sep. 2020, ISSN: 1432-0746.

[21] E. Di Valentino, A. Melchiorri, and J. Silk, "Planck evidence for a closed universe and a possible crisis for cosmology," *Nature Astronomy*, vol. 4, no. 2, pp. 196–203, 2020.

[22] Planck Science Team. (2013). "Planck CMB," [Online]. Available: `http://www.esa.int/Science_Exploration/Space_Science/Planck/Planck_and_the_cosmic_microwave_background` (visited on 05/05/2021).

[23] D. Perkins, *Particle Astrophysics*. Oxford University Press, 2008.

[24] P. J. E. Peebles and J. T. Yu, "Primeval adiabatic perturbation in an expanding universe," *The Astrophysical Journalm*, vol. 162, p. 815, Dec. 1970.

[25] WMAP Science Team. (2013). "Wmap data product images," [Online]. Available: `https://lambda.gsfc.nasa.gov/product/map/current/m_images.cfm` (visited on 05/05/2021).

[26] F. S. Queiroz, *WIMP theory review*, 2017. arXiv: `1711.02463 [hep-ph]`.

[27] M. Ackermann and al., "Dark matter constraints from observations of 25 milky way satellite galaxies with the Fermi large area telescope," *Phys. Rev. D*, vol. 89, p. 042 001, 4 Feb. 2014.

[28] C. Sivaram and K. Arun, *Some more exotic dark matter candidates: GUT balls, Fermi balls...* 2011. arXiv: `1109.5266 [physics.gen-ph]`.

[29] M. Schmaltz and D. Tucker-Smith, "Little Higgs theories," *Annual Review of Nuclear and Particle Science*, vol. 55, no. 1, pp. 229–270, 2005.

[30] R. N. Mohapatra, "Sterile neutrinos: Phenomenology and theory," *AIP Conference Proceedings*, vol. 478, no. 1, pp. 440–447, 1999.

[31] "A new era in the search for dark matter," *Nature*, vol. 562, no. 7725, pp. 51–56, 2018.

[32] S. Weinberg, "Approximate symmetries and pseudo-goldstone bosons," *Phys. Rev. Lett.*, vol. 29, pp. 1698–1701, 25 Dec. 1972.

[33] J. Goldstone, "Field theories with superconductor solutions," *Il Nuovo Cimento (1955-1965)*, vol. 19, no. 1, pp. 154–164, 1961.

[34] R. D. Peccei, "The strong CP problem and axions," in *Axions: Theory, Cosmology, and Experimental Searches*, M. Kuster, G. Raffelt, and B. Beltrán, Eds. Berlin, Heidelberg: Springer Berlin Heidelberg, 2008, pp. 3–17.

[35] M. E. Peskin and D. V. Schroeder, *An Introduction to quantum field theory*. Reading, USA: Addison-Wesley, 1995, ISBN: 978-0-201-50397-5.

[36] S. J. Brodsky, C. D. Roberts, R. Shrock, and P. C. Tandy, "New perspectives on the quark condensate," *Phys. Rev. C*, vol. 82, p. 022 201, 2 Aug. 2010.

[37] G. 't Hooft, "How instantons solve the U(1) problem," *Physics Reports*, vol. 142, no. 6, pp. 357–387, 1986, ISSN: 0370-1573.

[38] V. Baluni, "CP-nonconserving effects in quantum chromodynamics," *Phys. Rev. D*, vol. 19, pp. 2227–2230, 7 Apr. 1979.

[39] R. D. Peccei and H. R. Quinn, "CP conservation in the presence of pseudoparticles," *Phys. Rev. Lett.*, vol. 38, pp. 1440–1443, 25 Jun. 1977.

[40] ——, "Constraints imposed by CP conservation in the presence of pseudoparticles," *Phys. Rev. D*, vol. 16, pp. 1791–1797, 6 Sep. 1977.

[41] A. J. Powell, "The cosmology and astrophysics of axion-like particles," Ph.D. dissertation, Oxford U., 2016.

[42] K. Freese, J. A. Frieman, and A. V. Olinto, "Natural inflation with pseudo Nambu-Goldstone bosons," *Phys. Rev. Lett.*, vol. 65, pp. 3233–3236, 26 Dec. 1990.

[43] A. Ringwald, *Axions and axion-like particles*, 2014. arXiv: `1407.0546 [hep-ph]`.

[44] A. Einstein, *Quantentheorie des einatomigen idealen Gases: Abhandlung 2*. 1925.

[45] M. H. Anderson, J. R. Ensher, M. R. Matthews, C. E. Wieman, and E. A. Cornell, "Observation of Bose-Einstein condensation in a dilute atomic vapor," *Science*, vol. 269, no. 5221, pp. 198–201, 1995, ISSN: 0036-8075. DOI: `10.1126/science.269.5221.198`.

[46] "Observation of Bose-Einstein condensates in an Earth-orbiting research lab," *Nature*, vol. 582, no. 7811, pp. 193–197, 2020.

[47] K. Huang, *Statistical Mechanics*. 1963, pp. 477–483.

[48] L. Pitaevski and S. Stringari, *Bose-Einstein condensation and superfluidity*. Oxford University Press, 2016, pp. 9–10.

[49] O. Penrose and L. Onsager, "Bose-Einstein condensation and liquid helium," *Phys. Rev.*, vol. 104, pp. 576–584, 3 Nov. 1956.

[50] T. D. Lee, K. Huang, and C. N. Yang, "Eigenvalues and eigenfunctions of a Bose system of hard spheres and its low-temperature properties," *Phys. Rev.*, vol. 106, pp. 1135–1145, 6 Jun. 1957.

[51] L. Berezhiani, B. Famaey, and J. Khoury, "Phenomenological consequences of superfluid dark matter with baryon-phonon coupling," *Journal of Cosmology and Astroparticle Physics*, vol. 2018, no. 09, pp. 021–021, Sep. 2018.

[52] L. Berezhiani and J. Khoury, "Theory of dark matter superfluidity," *Phys. Rev. D*, vol. 92, p. 103 510, 10 Nov. 2015.

[53] "Particle densities for dilute hard-sphere Bose or Fermi gases in an external potential," *The European Physical Journal B - Condensed Matter and Complex Systems*, vol. 48, no. 3, pp. 385–391, 2005.

[54] D. Guerra, C. F. Macedo, and P. Pani, "Axion boson stars," *Journal of Cosmology and Astroparticle Physics*, vol. 2019, no. 09, pp. 061–061, Sep. 2019.

[55] J. Fan, "Ultralight repulsive dark matter and BEC," *Physics of the Dark Universe*, vol. 14, pp. 84 –94, 2016, ISSN: 2212-6864.

[56] S. Coleman, "Fate of the false vacuum: Semiclassical theory," *Phys. Rev. D*, vol. 15, pp. 2929–2936, 10 May 1977.

[57] C. G. Callan and S. Coleman, "Fate of the false vacuum. ii. first quantum corrections," *Phys. Rev. D*, vol. 16, pp. 1762–1768, 6 Sep. 1977.

[58] S. Coleman and F. De Luccia, "Gravitational effects on and of vacuum decay," *Phys. Rev. D*, vol. 21, pp. 3305–3315, 12 Jun. 1980.

[59] K. Olive, "Review of particle physics," *Chinese Physics C*, vol. 38, no. 9, p. 629, Aug. 2014.

[60] L. Hui, J. P. Ostriker, S. Tremaine, and E. Witten, "Ultralight scalars as cosmological dark matter," *Phys. Rev. D*, vol. 95, p. 043 541, 4 Feb. 2017.

[61] P. Zyla *et al.*, "Review of Particle Physics," *PTEP*, vol. 2020, no. 8, p. 083C01, 2020.

[62] H. J. Lane, "On the theoretical temperature of the Sun, under the hypothesis of a gaseous mass maintaining its volume by its internal heat, and depending on the laws of gases as known to terrestrial experiment," *American Journal of Science*, vol. s2-50, no. 148, pp. 57–74, 1870, ISSN: 0002-9599.

[63] C. G. Böhmer and T Harko, "Can dark matter be a Bose-Einstein condensate?" *Journal of Cosmology and Astroparticle Physics*, vol. 2007, no. 06, pp. 025–025, Jun. 2007.

[64] Y. Sofue, "Grand Rotation Curve and Dark-Matter Halo in the Milky Way Galaxy," *Publications of the Astronomical Society of Japan*, vol. 64, no. 4, Aug. 2012, 75.

[65] G. W. Hill, "On the part of the motion of the lunar perigee which is a function of the mean motions of the sun and moon," *Acta Math.*, vol. 8, pp. 1–36, 1886.

[66] E. Castellanos, C. Escamilla-Rivera, A. Macías, and D. Núñez, "Scalar field as a Bose-Einstein condensate?" *Journal of Cosmology and Astroparticle Physics*, vol. 2014, no. 11, pp. 034–034, Nov. 2014.

[67] T. Matos, E. Castellanos, and A. Suarez, "Bose-Einstein condensation and symmetry breaking of a complex charged scalar field," *The European Physical Journal C*, vol. 77, no. 8, p. 500, 2017.

[68] Y. Sofue and V. Rubin, "Rotation curves of spiral galaxies," *Annual Review of Astronomy and Astrophysics*, vol. 39, no. 1, pp. 137–174, 2001.

[69] F. Lelli, S. McGaugh, and J. Schombert. (2016). "Sparc database," [Online]. Available: `http://astroweb.cwru.edu/SPARC/` (visited on 10/10/2020).

[70] J. R. Brownstein and J. W. Moffat, "Galaxy rotation curves without nonbaryonic dark matter," *The Astrophysical Journal*, vol. 636, no. 2, pp. 721–741, Jan. 2006.

[71] F. Lelli, S. S. McGaugh, and J. M. Schombert, "The small scatter of the Baryonic Tully–Fisher Relation," *The Astrophysical Journal*, vol. 816, no. 1, p. L14, Dec. 2015.

[72] S. S. McGaugh and J. M. Schombert, "Color-mass-to-light-ratio relations for disk galaxies," *The Astronomical Journal*, vol. 148, no. 5, p. 77, Sep. 2014.

[73] R. Andrae, T. Schulze-Hartung, and P. Melchior, *Dos and don'ts of reduced chi-squared*, 2010. arXiv: `1012.3754 [astro-ph.IM]`.

[74] E. Castellanos, C. Escamilla-Rivera, and J. Mastache, "Is a Bose–Einstein condensate a good candidate for dark matter? a test with galaxy rotation curves," *International Journal of Modern Physics D*, vol. 29, no. 09, p. 2 050 063, 2020.

[75] J. Skilling, "Nested sampling for general Bayesian computation," *Bayesian Analysis*, vol. 1, no. 4, pp. 833 –859, 2006.

[76] J. I. Read, "The local dark matter density," *Journal of Physics G: Nuclear and Particle Physics*, vol. 41, no. 6, p. 063 101, May 2014.

[77] Harvard and Chandra X-ray observatory site. (2007). "Abell 520," [Online]. Available: `http://chandra.harvard.edu/photo/2007/a520/a520_comp.jpg` (visited on 05/05/2021).

[78] P. Sikivie, "Caustic rings of dark matter," *Physics Letters B*, vol. 432, no. 1, pp. 139–144, 1998, ISSN: 0370-2693.

[79] A. U. J. Lode, F. S. Diorico, R. Wu, P. Molignini, L. Papariello, R. Lin, C. Lévêque, L. Exl, M. C. Tsatsos, R Chitra, and N. J. Mauser, "Many-body physics in two-component Bose-Einstein condensates in a cavity: Fragmented superradiance and polarization," *New Journal of Physics*, vol. 20, no. 5, p. 055 006, May 2018.

[80] P. Bader and U. R. Fischer, "Fragmented many-body ground states for scalar bosons in a single trap," *Phys. Rev. Lett.*, vol. 103, p. 060 402, 6 Aug. 2009.